frontiers in Molecular Neuroscience

ORIGINAL RESEARCH
published: 26 November 2019
doi: 10.3389/fnmol.2019.00284

Transcriptional Profiling of Non-injured Nociceptors After Spinal Cord Injury Reveals Diverse Molecular Changes

Jessica R. Yasko[1], *Isaac L. Moss*[2] *and Richard E. Mains*[1]*

[1]*Department of Neuroscience, University of Connecticut Health Center, Farmington, CT, United States,* [2]*Department of Orthopedic Surgery and the Comprehensive Spine Center, University of Connecticut Health Center, Farmington, CT, United States*

Traumatic spinal cord injury (SCI) has devastating implications for patients, including a high predisposition for developing chronic pain distal to the site of injury. Chronic pain develops weeks to months after injury, consequently, patients are treated after irreparable changes have occurred. Nociceptors are central to chronic pain; however, the diversity of this cellular population presents challenges to understanding mechanisms and attributing pain modalities to specific cell types. To begin to address how peripheral sensory neurons below the injury level may contribute to the below-level pain reported by SCI patients, we examined SCI-induced changes in gene expression in lumbar dorsal root ganglia (DRG) below the site of injury. SCI was performed at the T10 vertebral level, with injury produced by a vessel clip with a closing pressure of 15 *g* for 1 min. Alterations in gene expression produce long-term sensory changes, therefore, we were interested in studying SCI-induced transcripts before the onset of chronic pain, which may trigger changes in downstream signaling pathways and ultimately facilitate the transmission of pain. To examine changes in the nociceptor subpopulation in DRG distal to the site of injury, we retrograde labeled sensory neurons projecting to the hairy hindpaw skin with fluorescent dye and collected the corresponding lumbar (L2–L6) DRG 4 days post-injury. Following dissociation, labeled neurons were purified by fluorescence-activated cell sorting (FACS). RNA was extracted from sorted sensory neurons of naïve, sham, or SCI mice and sequenced. Transcript abundances validated that the desired population of nociceptors were isolated. Cross-comparisons to data sets from similar studies confirmed, we were able to isolate our cells of interest and identify a unique pattern of gene expression within a subpopulation of neurons projecting to the hairy hindpaw skin. Differential gene expression analysis showed high expression levels and significant transcript changes 4 days post-injury in SCI cell populations relevant to the onset of chronic pain. Regulatory interrelationships predicted by pathway analysis implicated changes within the synaptogenesis signaling pathway as well as networks related to inflammatory signaling mechanisms, suggesting a role for synaptic plasticity and a correlation with pro-inflammatory signaling in the transition from acute to chronic pain.

Keywords: DRG, pain, inflammation, von Frey, hypersensitivity, FACS

OPEN ACCESS

Edited by:
Ildikó Rácz,
Universitätsklinikum Bonn, Germany

Reviewed by:
Edgar T. Walters,
University of Texas Health Science Center at Houston, United States
Rainer Viktor Haberberger,
Flinders University, Australia

***Correspondence:**
Richard E. Mains
mains@uchc.edu

Received: *21 August 2019*
Accepted: *08 November 2019*
Published: *26 November 2019*

Citation:
Yasko JR, Moss IL and Mains RE (2019) Transcriptional Profiling of Non-injured Nociceptors After Spinal Cord Injury Reveals Diverse Molecular Changes. Front. Mol. Neurosci. 12:284. doi: 10.3389/fnmol.2019.00284

INTRODUCTION

While spinal cord injury (SCI) is typically associated with loss of locomotor function, it can also result in chronic pain, affecting nearly 70% of patients with SCI (Finnerup et al., 2001). There are many categories of pain types affecting this population, however, studies indicate that neuropathic pain below, or distal, to the level of injury is among the most common and difficult to treat (Defrin et al., 2001; Finnerup et al., 2001; Siddall and Loeser, 2001; Yezierski, 2005; Nees et al., 2016). Of those patients reporting below-level neuropathic pain, half described their pain as severe or excruciating, causing significant disability in patients already disabled from loss of motor function (Defrin et al., 2001; Siddall et al., 2003). With few patients able to achieve complete relief with current treatment options, research has focused on mechanisms responsible for SCI pain at the site of injury, with the intention of treating the injury itself to prevent subsequent development of pain.

Considerable advances have been made in understanding changes within the spinal cord, including how spinally mediated alterations contribute to SCI-induced pain by increasing spinal cord excitability, and by establishing a variety of factors that impact how incoming sensory stimulation is processed (Bruce et al., 2002; You et al., 2008; Meisner et al., 2010). However, this approach has not translated into successful pain management. This may be attributed to an incomplete understanding of the differential functions of specific afferent subtypes in SCI, and how afferents distal to the site of injury become sensitized in patients with chronic below-level pain (Thakur et al., 2014). The sensory system receives inputs from multiple cell types, and peripheral cell bodies within the dorsal root ganglia (DRG) are important targets for assessing sensory function and pain (Usoskin et al., 2015). Persistent activity from injured and non-injured afferent fibers contributes to development and maintenance of many types of chronic pain (Devor, 2009; Gold and Gebhart, 2010; Walters, 2012).

Each sensory neuron has a unique pattern of gene expression that influences its modality-specific contribution to injury-induced pain (Le Pichon and Chesler, 2014). To better understand the underlying pathophysiology of below-level pain following SCI, it is necessary to identify changes in cells impacted by the injury. The skin is heavily innervated by a broad range of nociceptors, and previous work using a model of spared nerve injury (SNI) has shown that the function of cutaneous nociceptors can be impacted by injury (Berta et al., 2017). This has also been demonstrated in models of SCI by sustained spontaneous activity in peripheral terminals and in cell bodies of sensory neurons projecting to the skin after initial SCI (Carlton et al., 2009; Bedi et al., 2010; Wu et al., 2013; Yang et al., 2014; Ritter et al., 2015). Additional work has demonstrated that blockade of peripheral afferents into the central nervous system (CNS) can effectively mitigate patient discomfort and chronic pain (Campbell et al., 1988; Basbaum et al., 2009; Gold and Gebhart, 2010; Vaso et al., 2014; Haroutounian et al., 2018; Buch et al., 2019). These data support the idea that the mechanisms generating and maintaining prolonged pain reside within the peripheral nervous system.

In the present study, we identify specific transcriptional alterations in non-injured DRG distal to the site of injury. Using retrograde labeling from hairy hindpaw skin and flow cytometry, we isolated a nociceptor population projecting to sites distal to the spinal injury, free of surrounding neuronal and glial cells. This enabled identification of novel cutaneous nociceptor genes and predicted pathways not discernible by whole DRG tissue analyses.

MATERIALS AND METHODS

Animals

Experiments were conducted with adult (8–12 weeks) female C57BL/6J mice (Jackson Laboratory, Bangor, ME, USA). Several chronic pain conditions have a higher prevalence in females, and numerous studies have reported higher pain prevalence in the SCI population among female patients (Cardenas et al., 2004). Women also report greater frequency, severity, and longer-lasting pain, as well as neuropathic pain below the level of injury, in comparison to men (Cardenas et al., 2004). The majority of research examines SCI in male rodents and this study will add to what is known in the literature by focusing on female mice (Cardenas et al., 2004). Naïve animals were group-housed; sham and spinal cord injured animals were individually caged. All animals were maintained on a 12:12-h light-dark cycle with a temperature-controlled environment, and given food and water *ad libitum*. All treatments and testing were approved by the University of Connecticut Health Center Institutional Animal Care and Use Committee.

Spinal Cord Injury (SCI) Procedure

Animals were anesthetized by inhalation of isoflurane and a 1.0-cm dorsal midline skin sterile incision was made over T8–T11, as per Ma et al. (2001). Connective and muscle tissue were removed to expose the bone from T9–T10, and a laminectomy was performed at the T10 vertebral level. SCI was produced by compression of the vertical plane of the spinal cord using a vessel clip with a closing pressure of 15 *g* (WPI, Sarasota, FL, USA) for 1 min, exerting pressure from side to side on the spinal cord. Sudden impact is produced by the rapid release of the vessel clip (Tator and Poon, 2008). After removal of the clip a hemorrhagic ring at the site of compression is present. This injury is analogous to the majority of lesions in humans, as the model constitutes both contusion and compression (Marques et al., 2014). The injury resulted in paralysis of the hindpaws below the level of injury and was considered mild-moderate based on the ability of animals to exhibit slight ankle movement 24 h following injury (a score of 1 on the Basso Mouse Scale for locomotion), their ability to recover additional ankle movement by day 4, but the inability of mice to recover complete bladder control by day 4 (Basso et al., 2006). The wound is closed with coated vicryl absorbable sutures (Ethicon, Somerville, NJ, USA). Mice were allowed to recover in warm cages for 24 h. All animals were administered antibiotics once immediately following surgery (5 mg/kg gentamicin), as well as subcutaneous saline for 4 days following surgery, without analgesics. Sham control mice received the same treatment excluding the vessel

clip. Manual bladder expression on SCI mice was performed twice daily until mice were sacrificed. Mortality was less than 10% and typically occurred during the laminectomy due to excessive blood loss, or when postinjury weight loss required the animal to be sacrificed. Spinal cords collected at 4 days post-injury were most notably characterized by minimal cavitation and scar tissue that progressively diminished with increasing distance distal to the site of injury (∼L1–2 vertebral level), analogous to previous studies that have characterized this injury model (Joshi and Fehlings, 2002; Marques et al., 2014).

Behavioral Tests

Tail-Flick Test for Thermal Sensitivity

Mice were acclimated in 50 ml tubes for 2 days prior to testing, 20 min per day. On testing days, mice were left in their home cage to acclimate to the test room for 30 min before testing (Bannon and Malmberg, 2007). Latency to respond to thermal stimuli was measured by dipping the distal 1.5 cm of the tail into a 50°C water bath (Ramabadran et al., 1989). The tail was removed from the water upon response, or after 15 s to prevent tissue damage. The stimulus was conducted three times, at 20 s intervals or less (Zhou et al., 2014). The first response was dropped, and the average latency to respond from two trials was used for analysis. Video recording and VLC software were used to determine tail-flick responses in milliseconds. Mice were tested for thermal sensitivity 1 day prior to surgery for baseline response thresholds, and at days 1, 3, 5, and 7 post-surgery. $N = 6$ per group for each time point.

Mechanical Sensitivity

To assess mechanical sensitivity, mice were confined in clear plastic containers placed on an elevated wire mesh platform. Prior to testing, mice were acclimated to the apparatus for 60 min. Mechanical reactivity was assessed on the plantar surface of the hindpaw using a series of calibrated von Frey filaments according to the up-down method as described (Dixon, 1980), and 50% response thresholds were compared across all conditions. Both hindpaws were tested for mechanical sensitivity and collapsed across each group of mice per condition. Mice were tested for mechanical hypersensitivity 1 day prior to surgery for baseline response thresholds and at days 1, 3, 5, and 7 post-surgery. $N = 6$ per group for each time point.

Open Field Test

The open field test was conducted using a 16" × 16" open-field container subdivided by infrared beams to track movement (San Diego Instruments, San Diego, CA, USA). Data were acquired using the manufacturer's tracking software, which records ambulation movements based on beam breaks as well as central vs. peripheral beam break counts. All mice were placed in the same corner of the box before testing and allowed to freely explore for 10 min. Mice were tested 1 day prior to surgery for baseline locomotor behavior, and at days 1, 3, 5, and 7 post-surgery. Spinally injured mice were tested 1 day prior to surgery and 1 day post-surgery. Naive $N = 4$ for each time point; Sham $N = 3$–10 for each time point (within-group design, tissue was collected for ELISAs for corresponding time points); $N = 4$ SCI day 1.

Cuprizone Treated Mice

Female C57BL/6 mice (6–10 weeks old) were fed powdered milled chow mixed to contain a final concentration of 0.2% bis (cyclohexanone) oxaldihydrazone (cuprizone; Sigma-Aldrich, St. Louis, MO, USA), with food and water available *ad libitum*. Each mouse received approximately 5 g of chow per day, fresh cuprizone containing chow was prepared every 7 days. Cuprizone feeding was maintained for 35 days, and tissue was collected for protein analyses on day 35. Digitized, non-overlapping electron micrographs of the corpus callosum were analyzed for unmyelinated axon frequency and g-ratios to assess effectiveness of cuprizone treatment (Wasko et al., 2019; $N = 5$).

Cytokine ELISAs

Spinal cord segments at the level of laminectomy (T8–T11) were collected from naïve, sham, SCI, or cuprizone-treated mice immediately following perfusion with ice-cold 0.9% NaCl. Spinal cord segments were homogenized in ice-cold buffer containing 20 mM TES, pH 7.4, 10 mM mannitol, 0.3 mg/ml phenylmethylsulfonyl fluoride, 2 μg/ml leupeptin, 2 μg/ml pepstatin, 2 μg/ml benzamidine, 16 μg/ml benzamidine, and 50 μg/ml lima bean trypsin inhibitor at a concentration of 0.1 *g* tissue per 1 ml buffer (Mains et al., 2018). Homogenates were freeze-thawed three times, centrifuged (20 min, 17,400 *g*), and supernatants were collected. Approximately 60 μg of protein per sample was used for each ELISA. The ELISA assays were performed according to the manufacturer's instructions (R&D systems mouse duo-sets IL-10, IL-6, IL-1β, TNF-α, completed with Ancillary Reagent Kit 2, Minneapolis, MN, USA). The sample absorbance was read with an ELISA plate reader at 450 nm; readings were also taken at 570 nm to subtract optical background. The concentration was determined based on a standard curve. All results were normalized to amount of protein added per sample and graphed as pg/mg. Naïve, 1 day Sham, 4 days Sham, and 1 day SCI $N = 4$ mice; 5 days and 7 days Sham conditions $N = 3$ mice.

Backlabeling Procedure

To backlabel DRG L2-L6 projecting to the hairy hindpaw skin, mice were anesthetized with isoflurane. 0.3% wheat germ agglutinin conjugated to an AF-488 dye (WGA-488, Thermo Fisher Scientific, Waltham, MA, USA) in sterile PBS was injected into the sural, common peroneal, and saphenous nerve skin territories for retrograde labeling of DRG neurons (da Silva Serra et al., 2016; Berta et al., 2017). A total of 6 μl of WGA-488 was injected 2 days prior to surgery by three 2 μl injections in the lateral zones of each hindpaw (2 μl per nerve territory) using a 10 μl Hamilton Syringe and 30G needle. This was performed on both hindpaws of each mouse. This technique does not cause significant injury to the sensory afferents being studied.

Primary DRG Neuron Dissociation

Mice were anesthetized 4 days post-surgery with an intraperitoneal injection of ketamine (100 mg/kg) plus xylazine (10 mg/kg) and perfused with ice-cold 0.9% NaCl. A laminectomy was performed and L2-L6 DRG from both sides of the spinal column were collected into cold HBSS (KCl 5.4 mM,

NaCl 137 mM, Glucose 5.6 mM, Hepes 20 mM, pH 7.35 NaOH), after which the mice were sacrificed by decapitation. Sensory neuron dissociation was performed as described (Malin et al., 2007). Briefly, following collection, tissue was treated with 60U papain (Worthington), 1 mg of cysteine, and 6 μl of $NaHCO_3$ in 1.5 ml HBSS at 37°C for 10 min. Tissue was then treated with 12 mg collagenase II (Worthington, Lakewood, NJ, USA) and 14 mg dispase (Roche, Basel, Switzerland) in 3 ml HBSS at 37°C for 20 min, washed, and triturated with fire-polished glass Pasteur pipettes in 1 ml of DMEM (Gibco Thermo Fisher Scientific, Waltham, MA, USA) supplemented with FBS (Hyclone, Logan, UT, USA) and pen/strep (Gibco). The cell suspension was pelleted (1 min, 80 *g*), DMEM was removed, and cells were re-suspended in a modified solution (Citri et al., 2011) containing 140 mM NaCl, 5 mM KCl, 10 mM Hepes, 10 mM glucose, 0.1% Bovine Serum Albumin, pH 7.4. After re-suspension, cells were strained through a 70 μm cell strainer and placed on ice in the modified solution until fluorescence-activated cell sorting (FACS).

Imaging Flow Cytometry

Single cell suspensions of cells isolated from *in situ* WGA-488 labeled DRG were live-stained using Hoechst 33342 (10 μg/ml, Thermo Fisher Scientific, Waltham, MA, USA) and propidium iodide (PI; 1 μg/ml), and analyzed on an Amnis ImageStreamX Mark II imaging flow cytometer (Luminex Company, Austin, TX, USA). Fluorescent cell images were captured using a 60× objective lens with excitation from a 405 nm laser at 20 mW power and a 488 nm laser at 200 mW power. Images of in-focus nucleated WGA AF488-positive cells were identified and electronically gated using IDEAS software (Amnis, v6.2.183, Seattle, WA, USA).

Flow Cytometry and Cell Sorting

Neurons labeled with WGA-488 dye *in situ* in the DRG were purified by FACS 4 days post-surgery. Following primary dissociation of DRGs L2-L6, single cell suspensions were analyzed and sorted using a BD FACS Aria II cell sorter (Becton Dickinson) set up with a 130 μm nozzle at 12 PSI in order to gently isolate cells between 10 and 30 μm. Single live neurons were defined by electronic gating in FACS DIVA software (BD, ver. 8.01) using forward and side-angle light scatter, omission of PI (1 μg/ml), and AF488 fluorescence. All fluorescence gates were confirmed using fluorescence minus one controls (e.g., a sample of cells from unlabeled DRG was used to gate for AF488 positive cells and a sample of cells not treated with PI was used to set the live cell gate). WGA-488 positive cells were sorted directly into lysis buffer (NucleoSpin RNA XS Kit, Machery-Nagel, Bethlehem, PA, USA) and immediately placed on dry ice until RNA extraction. Cell sorting took 5–10 min per sample and was performed at 4°C before placement of samples on dry ice.

RNA Extraction and RNA Sequencing

RNA from FACS sorted cells was isolated using NucleoSpin RNA XS Kit, including a DNA digestion step but without carrier RNA step. Before library preparation, RNA quality and integrity was tested for each sample using the Agilent High Sensitivity RNA Screen Tape on the Agilent Tapestation 2200 (Agilent Technologies, Santa Clara, CA, USA). RNA with RIN values ≥6.7 (minimum 6.7, maximum 9.9, average 7.3) was further processed for RNA sequencing. It is important to note that these RIN values are based on relatively low RNA sample concentrations (RNA extracted from approximately 3,000 single cells per sample) and that the Agilent Tapestation software may have issues accurately calling RIN scores from sample concentrations below 50 ng/μl (Schroeder et al., 2006; Mueller et al., 2016). Because of this, RIN scores as low as 6.7 were considered suitable for RNA sequencing based on additional comparisons from the gel electrophoresis run on the Agilent Tapestation software that showed little to no RNA degradation, and previous work that has shown RNA samples with RIN scores below 7 are sufficient to identify differentially expressed genes (Gallego Romero et al., 2014). Library preparation was performed using the Illumina sequencing kit for high output 75-cycles for 25–30 M total single-end reads per sample. DESeq2 analyses[1] of differential expression were performed, and outliers beyond 30%–50% of the mean for each group of animals were eliminated (Love et al., 2014; Conesa et al., 2016; Labaj and Kreil, 2016; Wu and Wu, 2016).

Pathway Analysis

Data were analyzed by Ingenuity Pathway Analysis (IPA; Qiagen, Germantown, MD, USA). An overlap of significance for DEseq2 comparisons plus an RPKM cut-off >10 were required for transcripts to be included for IPA analysis. We analyzed 125 transcripts for comparisons between SCI and naïve groups, and 560 transcripts for comparisons between SCI and sham groups.

qPCR Validation

Pre-amplification of cDNA for Gene Expression

cDNA was generated from RNA samples from FACS sorted cells with the iScript Reverse Transcription Supermix (#1708840 Bio-Rad, Hercules, CA, USA), $N = 6$ per condition. Target-specific preamplification was performed on cDNA generated from RNA samples using SsoAdvanced PreAmp Supermix (#1725160 Bio-Rad) containing Sso7d fusion polymerase. Briefly, 20 μl of cDNA was pre-amplified in a total volume of 50 μl containing 25 μl of 2× SsoAdvanced PreAmp Supermix and 21 primer pairs, 50 nM of each primer. Preamplification was performed at 95°C for 3 min followed by 12 cycles of amplification at 95°C for 15 s and 58°C for 4 min. The samples were moved directly to ice and stored at −80°C. Pre-amplified cDNA was diluted 1:5 with H_2O. Controls performed for pre-amplification include qPCR and gel electrophoresis analysis of RNA extracted from both whole DRG tissue and FACS isolated DRG neurons from naïve mice. Following qPCR and gel analysis, all pre-amplified samples had no double bands and ran at expected weights based on product size.

qPCR

Following cDNA synthesis and preamplification, qPCR was performed using the primers listed in **Supplementary Figure S6**. All primers had calculated melt temperatures of 59.5–63.5°C,

[1] https://bioconductor.org/packages/release/bioc/html/DESeq2.html

and all products were 111–143 bp in length, as verified by agarose gel electrophoresis. Individual primers were analyzed by qPCR and gel electrophoresis from both whole DRG tissue and FACS isolated DRG neurons from naïve mice before pre-amplification was performed, to ensure proper primer efficiency. Following qPCR and gel analysis, all pre-amplified samples had no double bands, ran at expected weights based on product size, and had a maximum rate of amplification of 1.80/cycle or higher for all of the transcripts examined. qPCR was performed at 95°C, 2 min; 95°C, 10 s; 55°C, 15 s; and 72°C, 40 s, repeating the second through fourth steps for a total of 40 cycles in a Bio-Rad CFX Connect Optics Module machine. iQ SYBR Green Supermix (#1708882 Bio-Rad) was used for linear detection of qPCR results. Hypoxanthine phosphoribosyltransferase (Hprt) was used as the most constant normalizer transcript, based on the RPKM data (Klenke et al., 2016; Lima et al., 2016).

Statistical Analyses

Differences between groups were compared using student's *t*-test or ANOVA, followed by Tukey's post-test, Bonferroni's multiple comparisons test, or by unpaired student's *t*-test. *P*-values < 0.05 were considered statistically significant. Statistics on PCR data were conducted using delta CT values. Heat maps were generated by Microsoft software (Excel), hierarchical clustering was generated by Gene Cluster 3.0 and visualized using Java TreeView (de Hoon et al., 2004; Baek et al., 2017). All other data were plotted using Prism 6 (GraphPad Software, San Diego, CA, USA). R studio was utilized for differential expression analysis; Prism software was used for all other statistical tests.

RESULTS

Characterization of Behavioral and Inflammatory Phenotypes of Sham Mice

To determine an optimal time point to observe transcriptional changes contributing to the transition from acute to chronic pain, we tested behavioral differences between naïve and sham-operated mice. The objective of this was to ensure that changes within the DRG were due to injury to the spinal cord itself, not to the laminectomy performed in both injured and sham mice. It is likely that early effects of sham surgery involve changes in gene expression that overlap with a subset of genes that also change following SCI. It is important to define how long the functional effects of sham surgery persist to better discern the effects of SCI. Specifically, we tested naïve and sham mice for open field locomotor differences 1, 3, 5, and 7 days post-surgery (**Figure 1A1**). Naïve and sham mice did not differ significantly at any of the time points tested, including as early as 1 day post-surgery. To ensure that SCI mice (T10 compression-clip injury) did exhibit behavioral differences and locomotor deficits following injury, we compared SCI mice to naïve and sham mice for open field behavior 1 day post-injury (**Figure 1A2**). SCI mice exhibited substantially decreased total ambulation (one-way ANOVA, $p = 0.0059$, Tukey's multiple comparisons test, naïve $^{**}p < 0.005$, sham $^{*}p < 0.05$) following

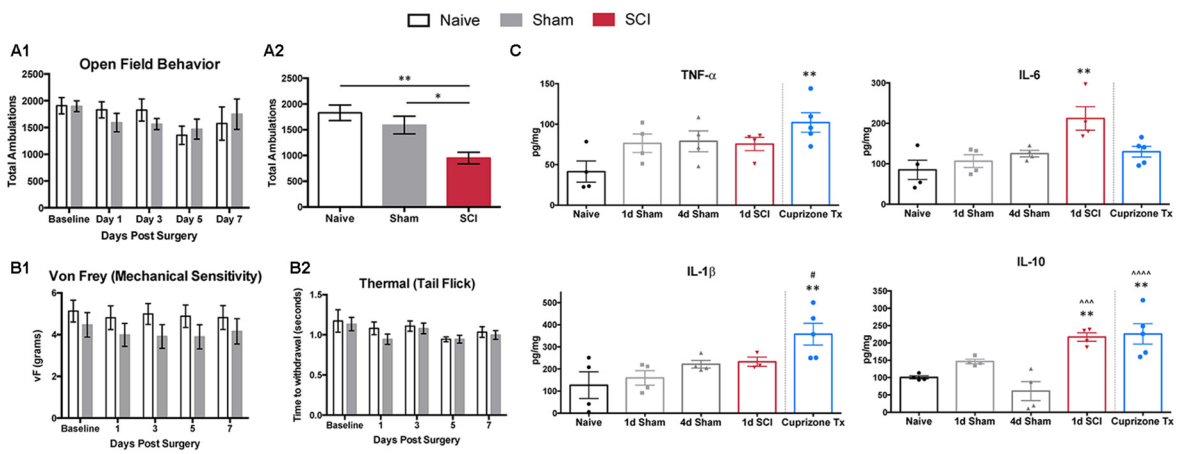

FIGURE 1 | Behavioral responses and cytokines. **(A1)** Open field behavior (10 min trials) in naïve or sham mice 0, 1, 3, 5 and 7 days post-surgery does not differ significantly at any time point in total ambulation, $N = 3$–10 sham, 4 naïve. **(A2)** Total ambulation differs significantly 1 day post-spinal cord injury (SCI) in both SCI vs. naïve (one-way ANOVA, $p = 0.0059$, Tukey's multiple comparisons test, $^{**}p < 0.005$) and SCI vs. sham ($^{*}p < 0.05$) mice. **(B1)** Mechanical and **(B2)** thermal sensitivity do not differ significantly 0, 1, 3, 5, and 7 days post-surgery in naïve and sham mice, $N = 6$ each. **(C)** Cytokine ELISAs on spinal cord segments at the level of laminectomy (T8–T11) show no significant differences between naïve and sham mice 1 or 4 days post-surgery. One-day post-operation, SCI mice have significantly increased levels of IL-6 and IL-10 compared to naïve controls (one-way ANOVA, Bonferroni's multiple comparisons test; $^{*}p < 0.05$, $^{**}p < 0.005$, respectively) and significantly increased levels of IL-10 in comparison to 4 days sham condition (one-way ANOVA, Bonferroni's multiple comparisons test; $^{\wedge\wedge\wedge}p < 0.001$). Cuprizone-treated mice as positive control, with significantly increased TNF-α, IL-1β, and IL-10 compared to naïve controls (one-way ANOVA, Bonferroni's multiple comparisons test; $^{*}p < 0.05$, $^{**}p < 0.005$, $^{\wedge\wedge\wedge}p < 0.001$, respectively) after 5 weeks of cuprizone treatment and significant increases in IL-1β at the 1 day sham time point, and IL-10 at the 4 days sham time point (one-way ANOVA, Bonferroni's multiple comparisons test; $^{*}p < 0.05$, $^{\wedge\wedge\wedge\wedge}p < 0.0001$, respectively). *Represents comparisons to naïve conditions, #represents comparisons to 1 day sham conditions, ^represents comparisons to 4 days sham conditions.

injury, as expected, although time spent in the periphery did not differ (**Supplementary Figure S1A**). Additional tests for mechanical (von Frey) and thermal (hot water tail-flick) hypersensitivity showed that naïve and sham conditions did not differ significantly at any time point (**Figures 1B1,B2**). Previous literature has demonstrated analogous results when testing hindpaw thermal sensitivity by radiant heat stimulus on sham animals at multiple time points (Christensen and Hulsebosch, 1997; Bedi et al., 2010; Gaudet et al., 2017). We did not examine SCI mice for thermal or mechanical sensitivity, as paralysis below the level of injury prohibited below-level sensitivity testing at the time points studied. Previous work using the clip-compression model has shown varying results regarding the occurrence of above-level sensitivity following SCI (Bruce et al., 2002; Densmore et al., 2010). While above-level pain may occur following injury, below-level pain is one of the most prevalent, and most difficult, pain types to treat, and is the focus of these studies (Yezierski, 2005). The development of chronic pain at later time points following clip-compression models of SCI (in addition to several other models) has already been well characterized. Therefore, we focused on early time points after injury, to identify contributions to the onset of pain, rather than changes after chronic pain has already developed (Bruce et al., 2002; Nakae et al., 2011; Gaudet et al., 2017).

Previous work has highlighted the importance of inflammatory cytokines within the CNS to facilitate the transduction of noxious stimuli in neuropathic pain (Cook et al., 2018). Thus, we examined post-surgical changes in inflammation, using ELISAs to analyze common cytokine markers to ensure that sham mice did not differ significantly from naïve mice following the removal of bone and muscle. We did not observe significant differences in inflammatory cytokine levels (TNF-α, IL-6, IL-1β, IL-10) in extracts of spinal cord segments (T8-T11) among naïve or sham mice at 1, 4, 5, and 7 days post-surgery (**Figure 1C**, **Supplementary Figure S1B**), similar to previous studies (Stammers et al., 2012). Spinal cords from SCI mice had significantly increased levels of IL-6 and IL-10 in comparison to naïve controls (one-way ANOVA, Bonferroni's multiple comparisons test; $^{*}p < 0.05$, $^{**}p < 0.005$, respectively). When compared to sham conditions, spinal cords from SCI mice had significantly increased levels of IL-10 in comparison to 4 days, 5 days, and 7 days sham conditions (one-way ANOVA, Bonferroni's multiple comparisons test; $^{***}p < 0.001$, $^{**}p < 0.005$, $^{**}p < 0.005$, respectively.

As a positive control, we tested cuprizone-treated mice (a model of multiple sclerosis), which are known to secrete proinflammatory cytokines at the end of 5 weeks of treatment (Mukhamedshina et al., 2017). Cuprizone-treated mice showed expected increases in levels of TNF-α, IL-1β, and IL-10 in comparison to naïve controls (one-way ANOVA, Bonferroni's multiple comparisons test; $^{*}p < 0.05$, $^{**}p < 0.005$, $^{**}p < 0.005$, respectively; Schmitz and Chew, 2008). Similarly, in comparison to sham mice, spinal cord extracts from cuprizone-treated mice had significant increases in IL-1β at the 1 day sham timepoint, and IL-10 at the 4 days, 5 days, and 7 days sham timepoints (one-way ANOVA, Bonferroni's multiple comparisons test; $^{*}p < 0.05$, $^{****}p < 0.0001$, $^{**}p < 0.005$, $^{***}p < 0.001$, respectively). Behavioral testing and cytokine analyses did not reveal differences between naïve and sham mice at any time point.

Confirmation of Cell Population Specific Labeling of Cutaneous Nociceptors

Because the laminectomy did not significantly affect behavior or inflammatory responses in sham mice, we determined an optimal time point to study the transition of acute to chronic pain based upon established characteristics of nociceptors following SCI. The inflammatory cytokine assays demonstrated significant increases in inflammation 1 day post-SCI compared to 4 days sham controls (**Figure 1C**, **Supplementary Figure S1B**). We did not observe significant differences in inflammatory cytokine levels (TNF-α, IL-6, IL-1β, IL-10) in extracts of spinal cord segments (T8-T11) among naïve or sham mice at 1, 4, 5, and 7 days post-surgery (**Figure 1C**, **Supplementary Figure S1B**); this is similar to previous studies (Stammers et al., 2012). In addition, previous studies have documented onset of spontaneous activity in nociceptors distal to the site of SCI as early as 3 days post-injury in rats; increased activity persisted for at least 8 months (Bedi et al., 2010). Thus, it is possible that the transition to chronic pain begins around 3 days after SCI in rats and mice, and this transition is not due to laminectomy, as nociceptors isolated from sham rats show either no significant changes in spontaneous activity (Bedi et al., 2010; Yang et al., 2014) or only a minor increase compared to the effect of SCI (Odem et al., 2018). Subsequently, we chose 4 days post-injury to assess transcriptional changes in nociceptors below the level of injury in mice.

To perform transcriptional profiling on nociceptors that project to the cutaneous skin after injury, we injected wheat germ agglutinin conjugated to an AF-488 dye (WGA-488) into the sural, common peroneal, and saphenous nerve skin territories for retrograde labeling of DRG neurons. Next, we performed compression-clip SCI or sham surgeries at the T10 vertebral level 2 days post-WGA injection and collected L2-L6 DRG for dissociation 4 days post-injury (**Figure 2A**). Based on the vertebral level at which we performed SCI, the DRG collected were located below the level of injury, thus our analysis was comprised of non-injured nociceptors that do not project directly to the lesion site. Flow cytometry confirmed that our cell population of interest (cutaneous nociceptors) was positively labeled with WGA-488 (**Figure 2B**). We also observed non-labeled (WGA-488) cells and dead cells (propidium iodide, PI+), to be excluded from cell sorting and analysis (**Figure 2B**). As expected, a significant number of viable small nociceptor cells were excluded in this analytical approach, to avoid including RNAs from non-nociceptor cells or attached fragments of dead cells (examples in **Figure 2C**; Thakur et al., 2014; Lopes et al., 2017; Megat et al., 2019).

FACS Purification of DRG Nociceptors Projecting to the Cutaneous Hind Paw

We performed FACS purification of nociceptor populations from naïve, sham, and SCI adult (8–12 weeks old) female

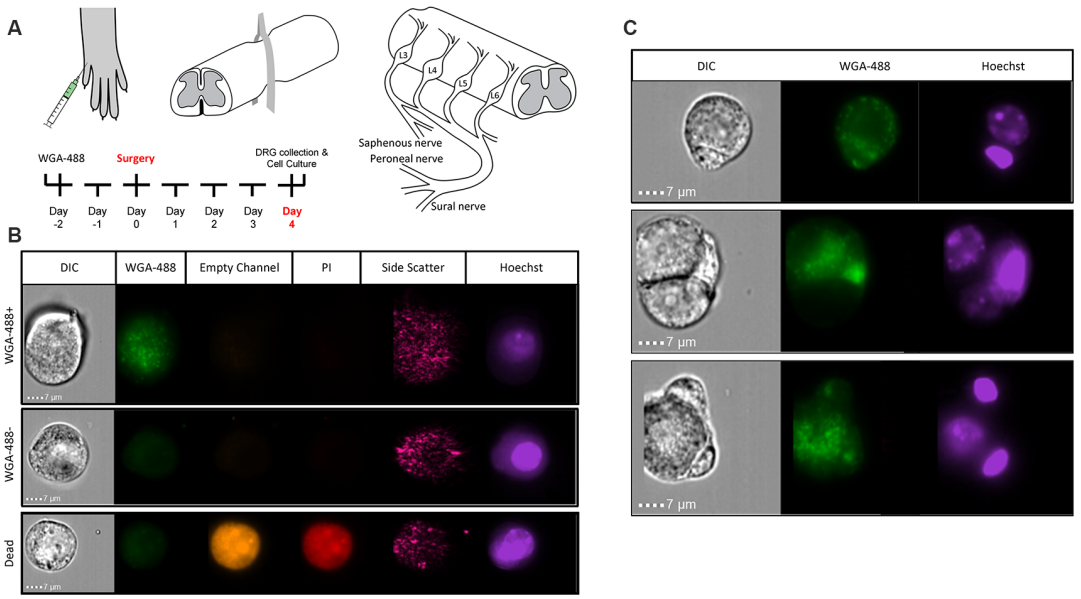

FIGURE 2 | Identifying sensory neurons. **(A)** Diagram of WGA-488 injection under the hairy hindpaw skin of a mouse, how the SCI was conducted with a vessel clip, and projections to the corresponding dorsal root ganglia (DRG). **(B)** Fluorescent cell images taken by Amnis ImageStreamX Mark II imaging flow cytometer (Luminex Corporation, Austin, TX, USA) using a 60x objective lens with excitation from a 405 nm laser and a 488 nm laser to identify propidium iodide (PI; red) positive (dead) cells and WGA (green) labeled cells, respectively. **(C)** Sample images of rejected cells because of attachment to non-nociceptor cells. Similarly, nociceptors with attached PI+ debris were eliminated.

mice (n = 5 per condition). We pooled DRGs from lumbar regions L2-L6 on either side of the spinal column to ensure all DRGs isolated would have projections to the hairy hindpaw skin. DRG cells were enzymatically dissociated and subjected to flow cytometry, to gently isolate positively labeled cells between 10 and 30 µm; PI staining was used to identify dead cells. All conditions were gated on DRG from naïve mice that did not receive WGA-488 injections, enabling purification of positively labeled cells (**Figure 3A**). Analysis of our flow cytometry data shows that, we were successful in retrogradely labeling DRG neurons projecting to hairy hindpaw skin. Many positively labeled neurons were part of cell aggregates, limiting retrieval of the single-cell population of interest to ∼2% of all dissociated cells per animal (**Figure 3B**). This percentage amounted to approximately 3,000 cells per mouse, a suitable representation of this cell population in agreement with previous studies (Shields et al., 2012; Goswami et al., 2014; Thakur et al., 2014; Usoskin et al., 2015; Berta et al., 2017). DRG populations were sorted directly into lysis buffer and placed on dry ice to preserve transcriptional profiles at the time of isolation. RNA quality was tested using the Agilent TapeStation; a representative image of an RNA sample following FACS purification is shown (**Figure 3C**).

Major Characteristics of Somatosensory Mediators in the Purified Neuron Population

We used the RNA sequencing data to evaluate the neuronal population that had been isolated. Scn10a, which encodes $Na_v1.8$, is present in 80–90% of nociceptors and Trpv1 serves as a marker for the peptidergic population of nociceptors (Basbaum et al., 2009; Harriott and Gold, 2009; Wu et al., 2013). RPKM values of 1,000 for Scn10a and 400 for Trpv1 confirm that FACS purified cells express high levels of these nociceptor markers **Figure 4A**). The low RPKM values observed for Parvalbumin (Pvalb), a glial transcript also found in large diameter proprioceptors and Aβ neurons, and glial fibrillary acidic protein (Gfap), another marker for glial cells, suggests that the non-nociceptive sensory neurons responsible for touch and proprioception (Aβ and Aδ neurons) and satellite glial cells are largely absent from our purified nociceptor population (**Figure 4B**; Huang et al., 2013; Le Pichon and Chesler, 2014); this conclusion is further supported by the somatosensory profiling of transcripts in **Figure 4C** (below). Previous studies have confirmed that intact DRG as well as unsorted dissociated DRG yield much higher levels of non-neuronal markers (Thakur et al., 2014). This highlights the importance of excluding cell aggregates during cell sorting (**Figure 3**) to avoid the analysis of transcripts from cells outside of the target population of nociceptors.

We next analyzed gene expression patterns for known functional mediators of somatosensation (Chiu et al., 2014; Le Pichon and Chesler, 2014; Usoskin et al., 2015). The purified cutaneous nociceptors displayed high expression levels of genes involved in thermosensation and nociception, such as specific Trp channels (notably Trpv1), sodium channels (Scn9a, 10a, 11a) and peripherin (Prph; **Figure 4C**). The skin is innervated by both peptidergic nociceptors and non-peptidergic neurons (Zylka et al., 2005; Lallemend and Ernfors, 2012; Kjell and Olson,

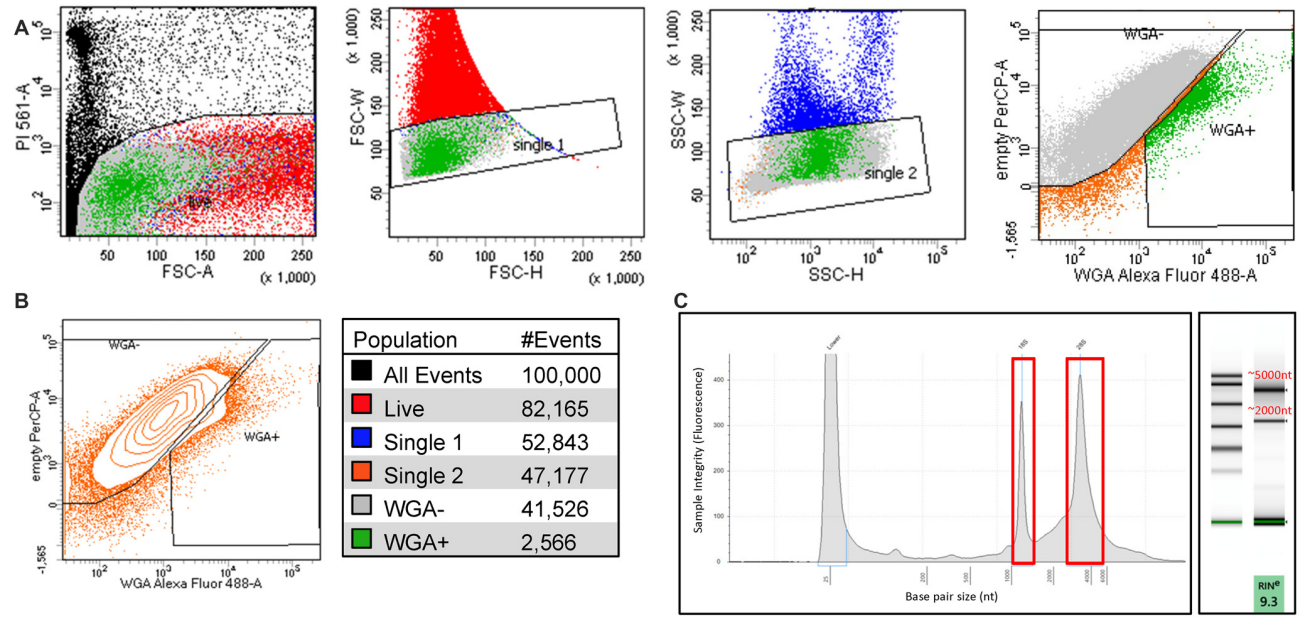

FIGURE 3 | Isolating sensory neurons. **(A)** Fluorescence-activated cell sorting (FACS) purification of cultured DRG cells based on PI staining (dead) single-cell populations by forward scatter (FSC), single-cell populations by side scatter (SSC), and cells fluorescently labeled with WGA-488 (WGA+). **(B)** Contour plot of single WGA+ cells that were sorted directly into lysis buffer for RNA extraction and color scheme for the gated populations, each condition $N = 5$; ~3,000 cells. **(C)** Representative image of RIN values run on an Agilent TapeStation before RNAseq.

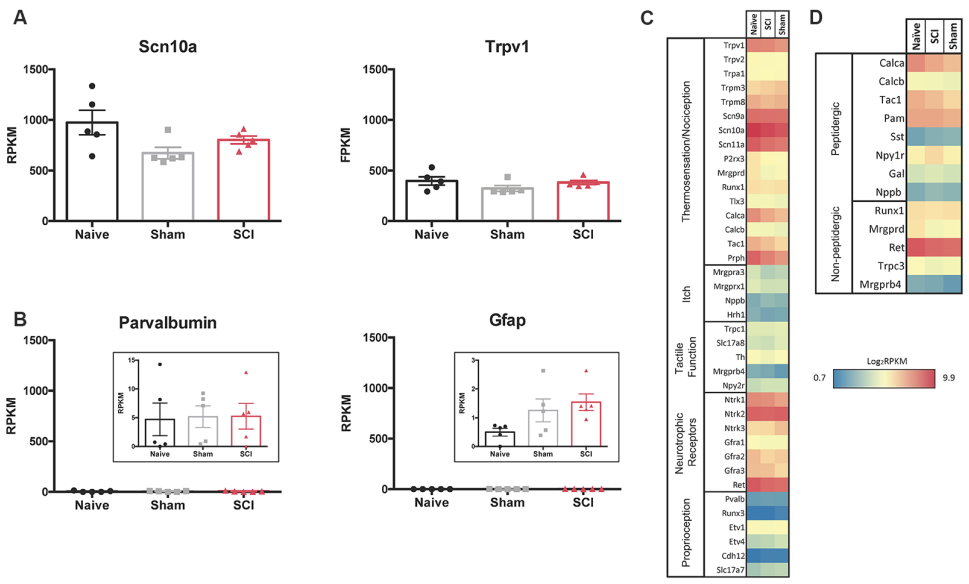

FIGURE 4 | RNAseq demonstrates specificity of cell isolation. **(A)** Average RPKM values from RNAseq dataset from genes that are known to be highly expressed in the cell population of interest or **(B)** expected to be expressed in other cell populations outside of the one being studied; larger myelinated neurons or satellite glial cells, respectively, $N = 5$ per condition. **(C)** Heatmap of functional somatosensory mediators within the isolated cell population of interest. Genes were grouped based on roles established in the literature: thermosensation and nociception, itch, tactile function, and neurotrophic factors. **(D)** Heatmap of peptidergic and non-peptidergic markers. Graph: $\log_2$ of average RPKM values within each condition, RPKM >1, $N = 5$ per condition.

2016). Markers for non-peptidergic nociceptors were abundant, such as Mas-Related G-Protein Coupled Receptor Member D (Mrgprd), Runt related transcription factor 1 (Runx1), Ret proto-oncogene (Ret), and transient receptor potential cation channel C3 (Trpc3). As expected, transcripts enriched in peptidergic nociceptors were present, such as Calca and

Calcitonin Related Polypeptides (Calcb) and Tac1 (the tachykinin precursor for peptides such as Substance P), the peptide processing enzyme peptidylglycine α-amidating monooxygenase (PAM), as well as Npy1r, one of the most abundant Npy receptors (Julius and Basbaum, 2001; Basbaum et al., 2009). However, genes encoding proteins involved in itch, such as brain natriuretic peptide (Nppb) and histamine receptor H1 (Hrh1) were only expressed at low levels (Usoskin et al., 2015). Similarly, genes responsible for proteins involved in tactile function, including Transient Receptor Potential cation channel subfamily C Member 1 (Trpc1), and those responsible for proprioception, such as Runt related transcription factor 3 (Runx3), exhibited low expression levels (Le Pichon and Chesler, 2014). In contrast, nerve growth factor receptors (Neurotrophic Receptor Tyrosine Kinases 1–3, Ntrk), which are characteristic of many subtypes of nociceptors, were expressed at high levels for each condition and did not differ significantly when comparisons were made between all conditions. It is of significance that Ntrk2 is typically used as a marker to identify myelinated sensory neurons, and relatively high levels of Ntrk2 (and Ntrk3) may indicate the presence of some proprioceptive or low threshold mechanoreceptors within the isolated population of neurons (Lallemend and Ernfors, 2012; Usoskin et al., 2015). However, this seems unlikely based on the absence of other common proprioceptor and mechanoreceptor transcripts within our dataset (**Figure 4C**). It is possible that higher levels of Ntrk2 and Ntrk3 are unique to our isolated population of neurons that project to the hairy hindpaw skin. High expression levels were also observed for some of the transcripts of the two major subpopulations of nociceptors: peptidergic and non-peptidergic (**Figure 4D**).

Gene Expression Profiling and Enrichment Patterns in Injured and Non-injured Cutaneous Nociceptors After SCI

To further assess expression profiles of the purified nociceptor population and differences among naïve, sham, and SCI conditions within this nociceptor-enriched population, we focused on expression patterns of gene families that mediate general neuronal functions (Chiu et al., 2014; Berta et al., 2017). We used differential expression analysis (DESeq2) to analyze significant changes between SCI and naïve or SCI and sham populations (Love et al., 2014). Pairwise comparisons of significant genes generated by DESeq2 analysis yielded many differentially expressed genes in each subset (**Supplementary Figures S2A,B**). We also assessed differences between sham and naïve populations. Any genes that differed significantly between the sham and naïve populations were considered significant transcript changes due to laminectomy, and thus were excluded from analysis in the SCI vs. Naïve and SCI vs. Sham comparisons (**Supplementary Figure S2C**).

We focused on expression patterns of gene families which mediate neuronal functions and contribute to pain phenotypes and found both high expression levels and significant differences within the chloride channel family, Trp channels, glutamate receptors, GABA receptors, potassium channels, sodium channels, and piezo channels (**Figures 5A–G**, *p*-values in **Table 1**). We also examined ASICs (acid-sensing ion channels), calcium channels, glycine receptors, and P2rx and P2ry families (purinergic receptors), because these are widely studied gene families known to be involved in the development or maintenance of chronic pain (**Supplementary Figures S3A–E**). Many channels and receptors were highly expressed within this cell population, but no significant changes among the transcripts were demonstrated for any condition (**Supplementary Figure S3**).

Several transcription factors were highly expressed, including signal transducer and activator of transcription 3 (Stat3), FJB osteosarcoma oncogene (Fos), and Jun Proto-Oncogene (Jun; **Supplementary Figure S4**). Evidence from various models of neuropathic pain implicates these transcription factors in the development or maintenance of chronic pain (Naranjo et al., 1991; Harris, 1998; Dominguez et al., 2008; Tsuda et al., 2011; Xue et al., 2014). Stat3 inhibitors are used to treat peripheral nerve injury-induced hyperexcitability within dorsal horn neurons, pain behaviors, chronic constriction injury, and signaling of IL-6 cytokines (Dominguez et al., 2008; Tsuda et al., 2011; Xue et al., 2014). Previous studies also show that Fos links extracellular events to long-term intracellular changes (such as noxious stimuli) and have established Fos expression as a valid tool to study nociceptive changes (Naranjo et al., 1991; Harris, 1998). Jun also contributes to persistent pain phenotypes following injury (Naranjo et al., 1991). DESeq2 analysis determined additional transcription factors to be significantly altered by SCI (**Supplementary Figure S5**). Interestingly, activating transcription factor-3 (Atf3), a cellular stress-inducible factor that also increases in non-injured neurons after axotomy, was present at similar levels as Atf4 in all conditions but did not differ significantly. This suggests that Atf3 may be upregulated by axonal injury during the DRG dissociation process, similar to other findings, but that the increases in Atf3 are not due to SCI itself (Tsujino et al., 2000; Huang et al., 2006; Seijffers et al., 2007).

Backlabeled FACS-Sorted Cutaneous Cell Transcriptome Is Distinguished by Nociceptor-Enriched Gene Patterns

To gain further insight into differentially regulated genes in our isolated population of neurons, we compared our dataset with similar studies on isolated DRGs from publicly available datasets which focused on nociceptors (expressing $Na_v1.8$) or DRG collected from the same lumbar spinal level (L2–L6; **Figure 6**; Thakur et al., 2014; Usoskin et al., 2015; Hu et al., 2016; Megat et al., 2019). Unsupervised hierarchical clustering of the top 260 genes revealed that a large number of genes display distinct patterns of expression dependent upon the technique used: isolated neurons from all DRG by translating ribosome affinity purification (TRAP) using the $Na_v1.8^{Cre}$ mouse (Megat et al., 2019); single-cell isolation from L3 to L5 DRG (Hu et al., 2016); single-cell isolation from L4-L6 DRG (Usoskin et al., 2015); and magnetic cell sorting (MACS) using the

TABLE 1 | Ion channels and synaptogenesis.

Gene	RPKM Naïve	RPKM SCI	RPKM Sham	*p*-value SCI vs. N	*p*-value SCI vs. Sham
Ion channels					
Calcb	86	83	71	-	6.5E-03
Gabrg3	12	6	17	5.3E-04	5.7E-04
Gfra2	219	166	186	1.3E-03	-
Gria4	108	131	119	5.0E-02	4.5E-02
Grik1	270	196	213	4.1E-05	-
Kcng3	20	13	18	3.3E-03	1.3E-02
Kcnh8	20	13	18	-	1.2E-02
Kcnj11	34	30	44	8.3E-04	-
Kcnk1	13	7	11	2.0E-02	1.7E-02
Kcnk13	28	19	30	-	2.2E-03
Kcnk18	19	15	23	3.2E-02	1.6E-03
Kcnn3	21	15	22	-	8.8E-03
Mrgprd	40	32	51	3.7E-07	-
Piezo2	143	82	96	1.5E-02	-
Scn3a	542	447	526	2.6E-02	1.0E-05
Scn5a	27	22	34	-	8.8E-04
Trpc3	23	17	34	5.2E-04	-
Trpc4	104	74	86	-	2.3E-03
Ttyh1	18	16	25	-	2.0E-02
Synaptogenesis pathway					
Adcy1	56	45	83	-	6.9E-05
Adcy2	120	144	140	2.9E-02	-
Ap2a2	307	305	260	-	1.6E-02
Atf4	154	147	121	-	1.3E-02
Bdnf	57	77	60	1.2E-02	3.6E-06
Cadm1	352	304	269	7.7E-02	4.5E-03
Camk2g	322	339	278	-	2.3E-02
Cdh10	35	34	46	-	9.0E-03
Dlg4	228	218	200	-	2.2E-02
Epha10	9	10	13	-	3.3E-02
Ephb2	11	9	15	-	8.4E-04
Gosr2	102	115	103	-	1.0E-02
Gria4	108	131	119	5.0E-02	4.5E-02
Nap1l1	210	203	177	-	3.1E-02
Nlgn2	202	205	185	-	9.4E-04
Plcg2	8	6	12	-	4.7E-04
Prkag2	161	169	147	-	5.7E-03
Prkar2b	182	153	147	1.5E-02	-
Rap2b	11	19	20	4.0E-03	-
Rasgrp1	364	286	303	8.1E-03	-
Rras	68	67	57	-	1.6E-02
Rras2	19	26	26	3.1E-02	-
Stxbp2	48	60	50	3.8E-02	3.0E-02
Syn3	28	27	37	-	4.0E-03
Syt4	235	231	197	-	1.1E-02

Average RPKM values that significantly differ 4 days post-spinal cord injury (SCI). DESeq2 p-Value based on SCI vs. naïve or SCI vs. sham comparisons. p-values that are not listed were >0.05. Transcripts from Ingenuity Pathway Analysis (IPA) canonical pathway analysis significantly different 4 days post-SCI. DESeq2 p-value based on SCI vs. Naïve or SCI vs. Sham comparisons.

$Na_V1.8$ TdTomato mouse (Thakur et al., 2014; **Figure 6A**). We found that, while our cutaneous nociceptor-enriched population clustered most closely with the datasets of both TRAP sorted and unsorted DRG from Megat et al. (2019), our isolated population was characterized by its own unique dataset. Notably, datasets from studies analyzing single-cell transcriptomes cluster together, while studies utilizing either TRAP or MACS cluster with their own respective unsorted DRG controls, suggesting that while techniques for isolating specific cell populations can be useful, some variations in gene expression may be attributed to individual differences in cell isolation and RNA extraction methods.

To better characterize enriched genes within our population, we graphed the expression of the 25 most significantly enriched genes in our dataset in comparison to the same datasets used for hierarchical clustering (**Figure 6B**). While many of the genes have similarly high expression levels, several genes were unique to our isolated population, including diacylglycerol kinase (Dgkh), ankyrin 2 (Ank2), PHD finger protein 24 (Phf24), serine/arginine repetitive matrix 2 (Srrm2), fatty acid synthase (Fasn), phosphoinositide-interacting regulator of transient receptor potential channels (Pirt), and pleckstrin homology domain containing, family A member 6 (Plekha6). We also compared the expression pattern of

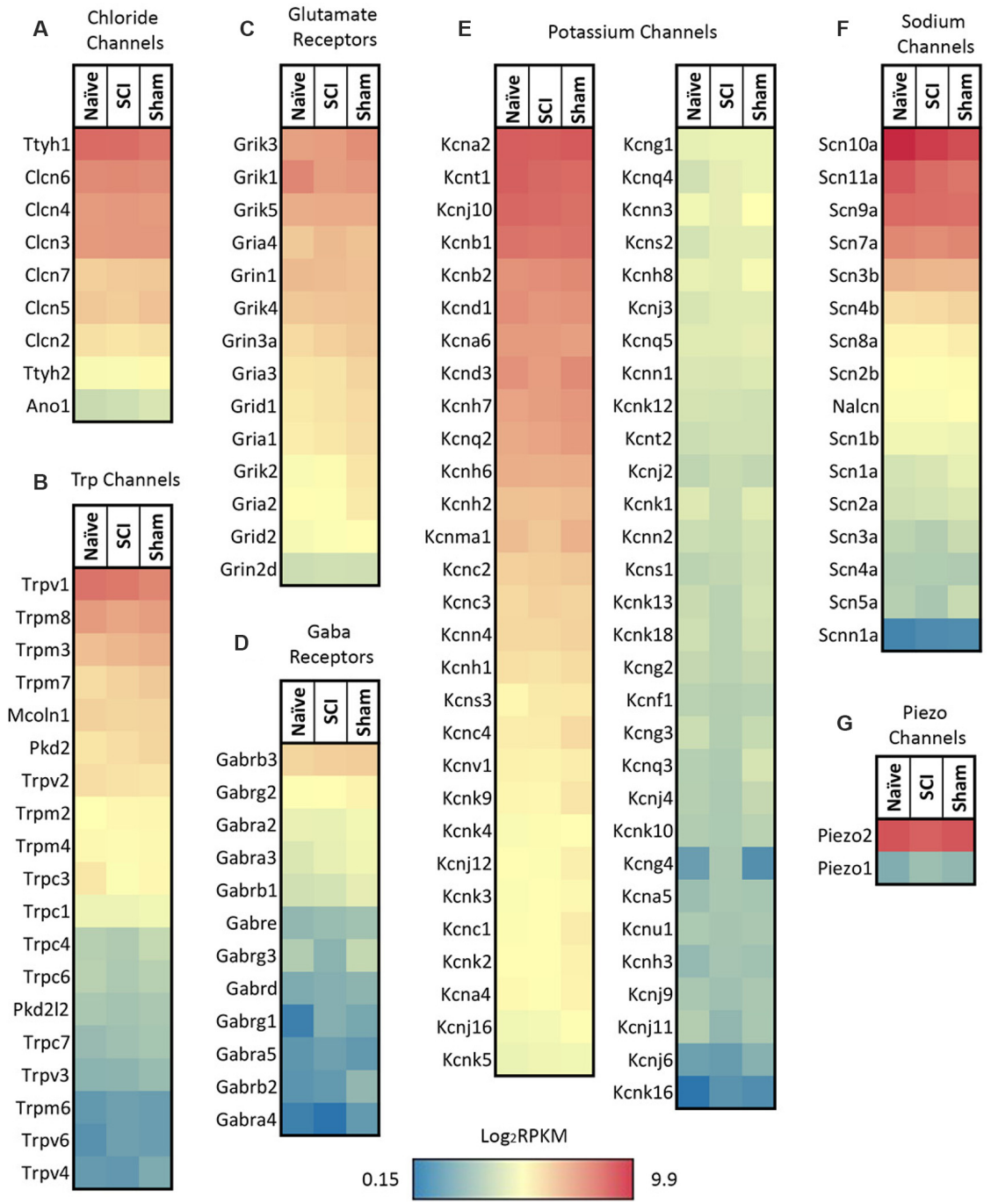

FIGURE 5 | Heatmaps of ion channel transcripts. **(A)** Chloride channels, **(B)** TRP channels, **(C)** glutamate ionotropic receptors, **(D)** GABA ionotropic receptors, **(E)** potassium channels, **(F)** sodium channels, **(G)** piezo channels. Each family of transcripts includes significant differences in at least one gene 4 days post-SCI. Channels were clustered based on SCI expression level and graphed by the $\log_2$ of average RPKM values within each condition. RPKM <1 were not included, $N = 5$ per condition.

our naïve nociceptor-enriched population to the various datasets by again examining known neuronal markers of somatosensation (**Figure 6C**). As predicted, all of the sorted populations exhibit relatively high expression levels of gene transcripts associated with thermosensation, nociception, or neurotrophic receptors, and comparatively low levels of genes associated with itch, tactile function, or proprioception. It is evident that our cutaneous, nociceptor-enriched population can be defined by its distinct gene expression patterns, in particular, high expression levels of the Trp family of genes

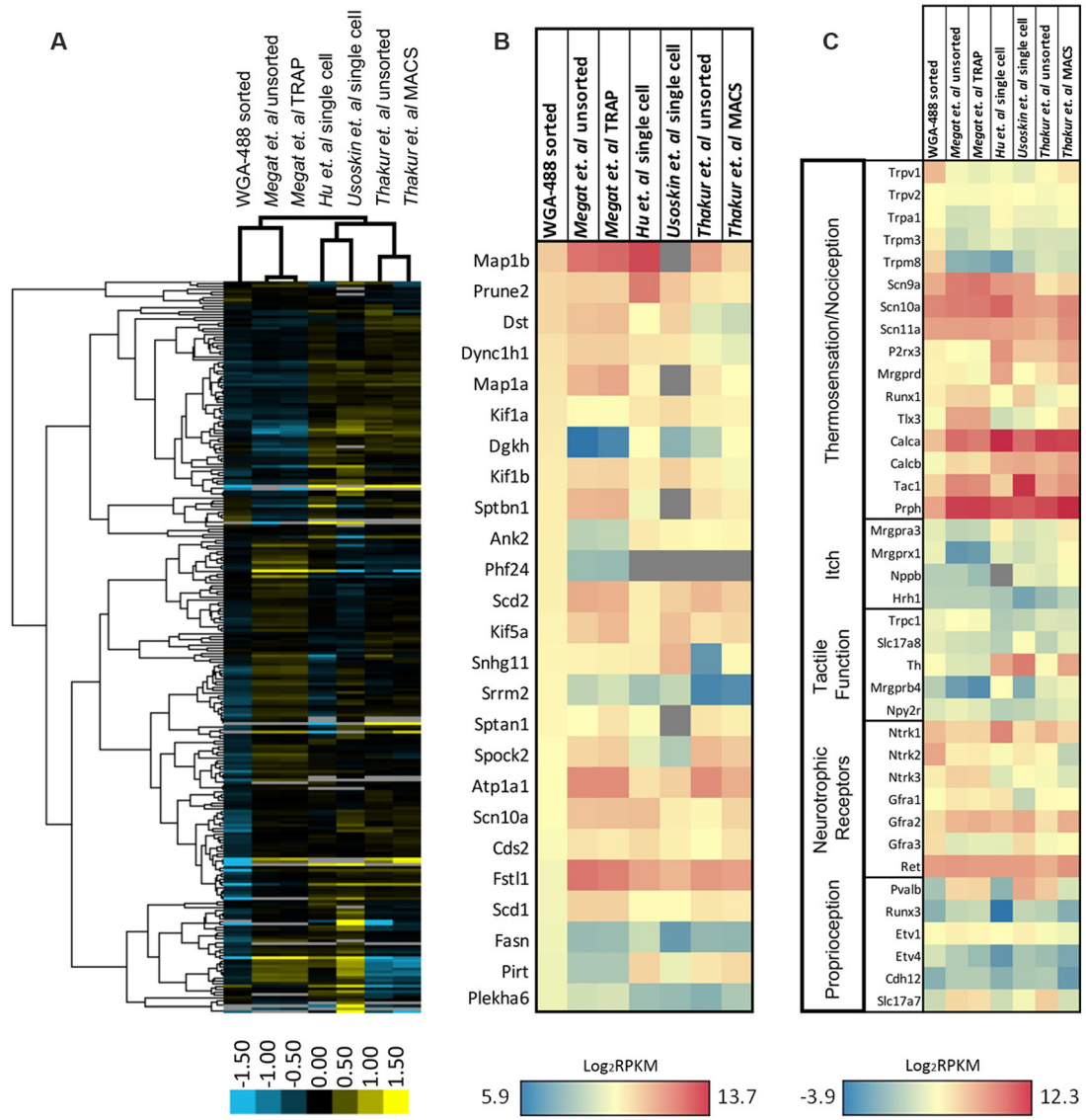

FIGURE 6 | Expression profiling of differentially sorted isolated DRG. **(A)** Heatmap of the top 260 genes from sorted isolated DRG neurons in comparison to similar studies from publicly available datasets (unsorted dissociated DRG, translating ribosome affinity purification (TRAP)-sorted, single cell, or MACS-sorted dissociated DRGs). Comparisons between conditions were made by unsupervised hierarchical clustering. **(B)** Heatmap of the 25 most significantly enriched genes in our dataset in comparison to similar studies from publicly available datasets. Transcripts were graphed by the $\log_2$ average values within each condition. Datasets that did not express transcripts (RPKM = 0) are depicted in gray. **(C)** Heatmap of functional somatosensory mediators within the isolated cell population of interest in comparison to similar studies from publicly available datasets. Transcripts were graphed by the $\log_2$ average values within each condition. Datasets that did not express transcripts (RPKM = 0) are depicted in gray.

listed in **Figure 6C**, as well as Ntrk2, Ntrk3, and Gfra3 neurotrophic receptors.

Ingenuity Pathway Analysis (IPA) Identified Significantly Different Canonical Pathways From Cutaneous Nociceptors After SCI

Based on DESeq2 analysis, levels of several hundred transcripts in the nociceptor-enriched population were altered by SCI. We restricted IPA input lists to genes that had RPKM values greater than 10 and were statistically different (SCI vs. Naïve or SCI vs. Sham) by DESeq2 analysis (**Figures 7A,B**). Transcripts that exhibited large-fold changes included Mrgprb5, Hal, Chrnb4, Cap2, Sez6l, Calb1, Prokr2, Rxfp1, Nxpe2, and Arap3 (**Figures 7A,B**). Despite the noticeable changes in these individual genes, they did not appear in any common significant canonical pathways. Instead, we chose to focus on smaller-fold changes that may result in the coordinated functions of many genes. IPA identified several pathways that are considered important for inflammatory processes, pain transduction, or

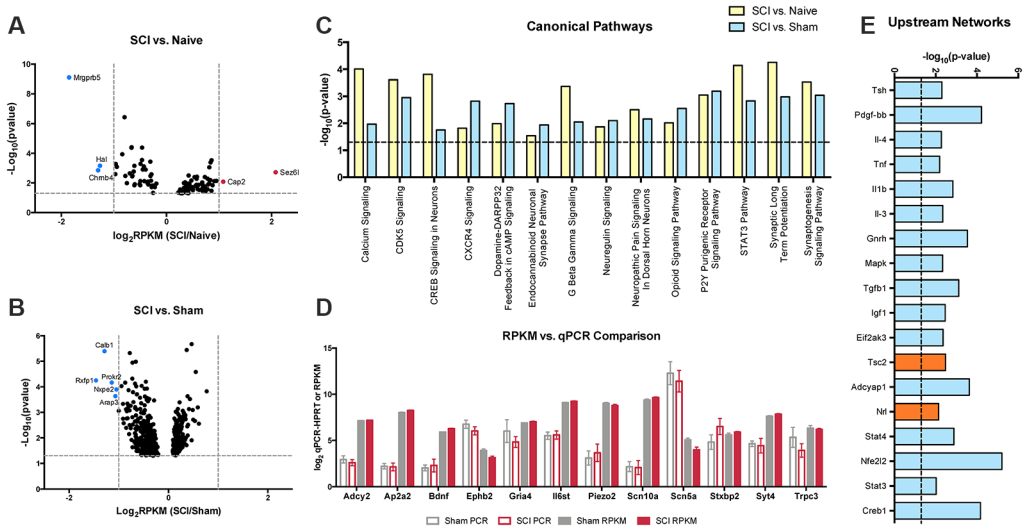

FIGURE 7 | Volcano plots and upstream analysis. **(A,B)** DESeq2 significant ($p > 0.05$) genes included in IPA analysis comparing SCI vs. naïve or SCI vs. sham conditions. **(C)** Significant ($p < 0.05$) overlapping canonical pathways predicted by analyzing genes determined by DESeq2 and outlier cut-off in IPA. **(D)** Comparisons of RPKM values generated by RNAseq and log2 transcript levels (gene-Hprt) validated by qPCR between sham and injured conditions. **(E)** IPA network analysis predicted networks based on differentially expressed genes between sham and SCI conditions. Network analysis also made predictions about the activation state of the transcript regulator; positive *z*-score (blue) indicates activation, negative *z*-score (orange) indicates inhibition.

the maintenance of chronic pain (**Figure 7C**). This includes calcium signaling, Cxcr4 signaling, neuropathic pain signaling in dorsal horn neurons, opioid signaling, purinergic receptor signaling and synaptic long term potentiation (**Figure 7C**; Julius and Basbaum, 2001; Walters, 2012, 2018). The current study focused on significant changes due to SCI pain and not due to post-surgical pain (i.e., changes between sham vs. naïve groups).

Validation of RNASeq Data Using qPCR

We used qPCR to confirm changes in transcripts of interest from our RNAseq dataset. To validate qPCR and RNAseq comparisons, we compared qPCR or RPKM Log_2 transcript levels of SCI and sham genes of interest (**Figure 7D**). SCI and sham qPCR fold change results were analogous to the RNAseq fold change dataset. We focused on the synaptogenesis pathway in particular, as it includes several genes present in overlapping canonical pathways, including changes in receptors involved in organization of excitatory signaling (Ephb) and synapses which may be involved in development of chronic pain (TrkB and BDNF). We validated receptors for significant genes in the synaptogenesis pathway, and genes considered possible contributors to pain that also showed significant differences between conditions Gabrg3, Il6st, Kcng3, Piezo2, Scn5a, Trpc3; Waxman et al., 1999; Wickenden, 2002; De Jongh et al., 2003; Devor, 2006; Eijkelkamp et al., 2013; Guptarak et al., 2013; Xia et al., 2015; Deng et al., 2018; Szczot et al., 2018). Additional targets were chosen in order to validate isolation of the correct cell population (Scn10a). Samples for qPCR were collected by backlabeling cutaneous afferents and cell sorting, consistent with samples generated for RNAseq analysis. Following cDNA synthesis, samples were subjected to gene target-specific preamplification using the same primers used for qPCR (**Supplementary Figure S6**). Hprt was chosen as the housekeeping gene for qPCR analysis because it was the most constant normalizer transcript from the RPKM data across all 15 mice in the present study (Klenke et al., 2016; Lima et al., 2016).

IPA Network Analysis Revealed Several Regulatory Interrelationships After SCI

We used IPA upstream network analysis to further interpret the function of the several hundred transcripts significantly altered determined by DESeq2. This method predicted several transcriptional regulators associated with altered expression levels of downstream target genes following SCI (**Figure 7E**). The upstream regulator molecules graphed do not show a significant change in RNA expression in response to injury. However, these targets are activated by posttranslational modifications that can alter many of the downstream molecules within its network.

DISCUSSION

SCI initiates persistent molecular changes in nociceptors, similar to inflammation in models of peripheral injury (Djouhri et al., 2001; Xie et al., 2005). Several studies of SCI pain have evaluated mechanical hypersensitivity from von Frey stimulation above and below the level of thoracic injury, in addition to testing tail withdrawal from heat stimuli (Kramer et al., 2017; Shiao and Lee-Kubli, 2018). Additional behavioral studies have demonstrated that SCI animals exhibit significant increases in mechanical and thermal hypersensitivity compared to naïve and sham animals, beginning at 1 month and persisting for several months

post-injury (Carlton et al., 2009; Bedi et al., 2010). However, other studies have asserted that operant behavioral tasks, such as conditioned place preference, are required to effectively study spontaneous pain in animals with SCI (Yezierski, 2005; Davoody et al., 2011; Yang et al., 2014). The present study focused on the transition from acute to chronic pain, in the absence of early pain-related behavior, to examine transcriptional differences that occur at much earlier time points rather than a point at which chronic pain is already present. We first tested behavioral differences between naïve and sham mice to identify changes due to the laminectomy, not the SCI itself, to better determine a time point that captures the transition from acute to chronic pain following SCI. For example, removal of bone and muscle alone could trigger chronic pain-like symptoms, analogous to post-surgical pain reported in humans (Woolf, 2011). Sham surgery for SCI has also recently been reported to produce significant increases in pain-avoidance behavior in rats, which is indicative of persistent post-surgical pain (Odem et al., 2019). Surprisingly, there were no significant differences between naïve and sham mice at any time point (**Figures 1A,B**), suggesting that the laminectomy did not produce any locomotor differences or behavioral hypersensitivity 1–7 days post-surgery in mice. By contrast, the SCI produced clear locomotor differences (**Figure 1A2**).

Injury and Inflammation in SCI

We also considered post-surgical inflammation, using cytokine ELISAs to assess changes in the spinal cord at the level of laminectomy (T8–T11). We wanted to assess changes in cytokine levels for two main reasons; first, to confirm that sham mice did not exhibit differences from naïve mice at key time points in comparison to SCI mice, and second to determine whether sham mice exhibited a prolonged inflammatory response, which could potentially be correlated to the development of chronic pain (Guptarak et al., 2013; Krames, 2014). Both pro-inflammatory cytokines TNF-α and IL-1β have been studied in neuroprotection models of SCI. IL-6 has been implicated in neurodegeneration after CNS injury, and the anti-inflammatory cytokine IL-10 exhibits neuroprotective effects (Donnelly and Popovich, 2008; Schmitz and Chew, 2008; Zhang et al., 2019). However, we did not find any significant cytokine changes between naïve and sham mice within 7 days of injury, indicating that the laminectomy did not produce a significant inflammatory response at the time points tested. As a positive control for the cytokine ELISAs (Suzuki and Kikkawa, 1969), we used the cuprizone model for multiple sclerosis. Key pathological features of the treatment include secretion of proinflammatory cytokines such as TNF-α and IL-1β (Schmitz and Chew, 2008). Consistent with previous findings, mice treated with cuprizone exhibited significant increases in TNF-α, IL-1β, and IL-10 relative to naïve mice (**Figure 1C**; Schmitz and Chew, 2008).

Tissue injury can also lead to prolonged functional changes and hyperalgesia that are accompanied by behavioral changes due to increased spontaneous activity of nociceptors (Carlton et al., 2009; Bedi et al., 2010; Walters, 2012). Spontaneous activity in nociceptors following SCI begins at 3 days after injury and persists for at least 8 months (Bedi et al., 2010). This increase in nociceptor activity elicits changes within the spinal dorsal horn, which receives input from these nociceptors, ultimately contributing to spontaneous pain (Dubner and Ruda, 1992; Wu et al., 2001). However, the source of hyperexcitability of nociceptors after injury is still unknown. Because spontaneous activity in nociceptors begins by 3 days post-injury, and has been correlated with the generation of persistent pain, we chose to observe transcriptomic changes immediately after this time point at 4 days post-injury (Xie et al., 2005). We intentionally excluded large sensory afferents from our experimental model, as the response to SCI by these afferents is transient and large sensory afferents have not been directly correlated with pain transduction in other models of chronic pain (Huang et al., 2006; Hu et al., 2016). We focused on an anatomically defined population of nociceptors (projecting from below the level of SCI to hairy hindpaw skin) by backlabeling from peripheral afferent terminals and sorting based on both fluorescence and size. These neurons represent ∼10% of dissociated DRG tissue and have a distinct transcriptome (Thakur et al., 2014). Our approach to identifying anatomically defined small nociceptors is distinct from single-cell transcriptome isolation based on the expression of the sodium channel Scn10a ($Na_v1.8$) or expression of advillin (Avil, a marker for all neural crest neurons; Lopes et al., 2017; Megat et al., 2019).

Different DRG Neuronal Populations in SCI

Different types of sensory neurons are distinct in their responses to injury. It is likely that, even within an identified subpopulation, cells will nonetheless exhibit heterogeneity (Hu et al., 2016). Because injury does not impact all afferents in the same way, we analyzed gene expression changes within the population of nociceptors projecting to the skin below the level of injury. By focusing on small nociceptors innervating dermatomes below the level of injury, we begin to address what unique set of genes within a specific population may be contributing to the burning, stabbing, and shooting pain reported in SCI patients suffering from below-level neuropathic pain (Siddall et al., 2003). Our goal was to better understand how SCI affects molecular changes within a specific population of neurons, and how this may contribute to hypersensitivity following SCI. We focused our analysis on sensory neurons from lumbar DRGs (below the level of the SCI) projecting to the hairy hindpaw skin (**Figure 2A**). After confirming, we had isolated the cell population of interest (**Figures 2B**, **3**), we used RNAseq to identify changes in gene expression. The use of RNA-Seq has clear advantages over microarrays, since RNA-Seq is not limited to a set of pre-determined transcripts, has a larger dynamic range of transcript expression, and is highly reproducible (Usoskin et al., 2015). By utilizing this technology, we were able to identify transcript changes undetectable with traditional RT-PCR or microarrays (Wang and Zylka, 2009). Our RNAseq data from naïve, sham, and injured animals display distinct patterns of somatosensory genes present in this nociceptor-enriched population. In particular, RPKM values show high levels of Scn10a (a marker for nociceptors), purinergic receptor P2rx3, Mrgprd (markers for the non-peptidergic population of nociceptors), and Calca and Calcb (neuropeptide precursors), indicating that we isolated the desired nociceptor specific cell

population, and also indicating important genes within the population of sensory neurons projecting to the hairy hindpaw skin (**Figures 4A–D**). Multiple gene transcripts important for itch, tactile function, and proprioception all had relatively low RPKM values, indicating again that we isolated the desired target cell population, and that injury did not induce modifications in the type of stimuli nociceptors transduce (**Figure 4C**). Our population-level analysis revealed significant changes after SCI in a number of ion channels and receptors that are already known to play a role in pain or hypersensitivity, such as Piezo2, and transcripts involved in excitatory signaling, such as Grik1 (**Figure 5C**, **Table 1**). However, there were also many genes whose expression and functional roles in persistent pain have yet to be characterized, including Trpc4 and Ttyh1 (**Figures 5A,B**, **Table 1**).

Transcriptome Profiling in Studies of DRG

Many studies have utilized RNA-seq technology to gain insight into nociceptor transcriptomes within the DRG and how it changes relative to different pain models (Thakur et al., 2014; Usoskin et al., 2015; Hu et al., 2016; Megat et al., 2019). Although previous screens have yielded various nociceptor-specific genes, we have identified a unique pattern of gene expression within a population of nociceptors projecting to the periphery (**Figure 6**). By cross-comparing our dataset with similar studies, we were able to identify our cells of interest and confirm that, we obtained cell-type specificity. Notably, many of the current technologies require a transgenic mouse with a cell-type specific reporter. However, by taking advantage of the anatomical organization of the mouse, we were able to use backlabeling and FACS sorting in non-transgenic animals to isolate a nociceptor-enriched population with a low degree of contamination with other cell types. We further implemented this methodology to identify candidate genes in a specific population of neurons below the level of injury in a model of SCI to better understand the heterogeneous injury response among the many subtypes of DRG neurons.

Among these comparisons, we observed large fold changes in several genes (**Figures 7A,B**, highlighted in red and blue). However, instead of focusing on larger changes in a small subset of genes with individual functions, we concentrated our analysis on the interaction of many transcripts that were significantly altered after SCI and how these influenced intracellular signaling pathways (**Figure 7C**). Ingenuity Pathway Analysis implicated numerous pathways associated with the progression to persistent pain. We took particular interest in the synaptogenesis signaling pathway as a key player at this 4-day time point, suggesting a role for synaptic plasticity in the transition from acute to chronic pain after SCI. In addition to its relevance within our model, many of the transcripts involved in synaptic plasticity overlapped with several other pathways (**Figure 7C**) and had RPKM values that could be validated by qPCR (**Figure 7D**). Synaptogenesis is typically associated with developmental processes, including axon guidance and synapse formation (Klein, 2004; Price and Inyang, 2015). However, activation of various signaling pathways involved in synaptogenesis may also contribute to pain; for example persistent pain is supported *via* changes in synaptic signaling, neuronal plasticity, and long term potentiation, and may form memory-like networks for painful signals that allow persistent pain to occur long after the initial injury (Kobayashi et al., 2007; Khangura et al., 2019).

Included in the many of the genes of interest within the synaptogenesis pathway, Ephb2 was significantly down-regulated post-injury (**Table 1**). The gene transcript is part of the Ephrin tyrosine kinase receptor protein family that is expressed in laminae I-III of the spinal dorsal horn on small and medium-sized DRG neurons (presumably nociceptors; Bundesen et al., 2003). Ephb receptors regulate synaptic activity in the spinal cord and contribute to persistent pain associated with NMDA activity (Khangura et al., 2019). Numerous receptor tyrosine kinases localize to synapses and contribute to synaptogenesis in addition to EphB receptors, including Trk receptors (Biederer and Stagi, 2008). Ntrk2, the receptor for BDNF, was highly expressed in this cell population; commensurately, BDNF transcript levels were significantly upregulated in the injured population (**Table 1**). Camk2g transcript levels were significantly increased in the SCI population of cutaneous nociceptors as well, and recent work has shown phosphorylation of Camk2g induces Bdnf mRNA transcription (Melemedjian et al., 2013; Yan et al., 2016). This parallels increasing evidence that neuronal activity (such as increased activity or hyperexcitability) activates alternative neuronal circuits through activity-regulated genes, such as *BDNF* (Lu et al., 2009; Melemedjian et al., 2013). Many of the genes significantly altered in the synaptogenesis pathway may function together to generate neuropathic pain (**Supplementary Figure S7**).

Networks of Genes Coordinating Responses to SCI

Regulatory interrelationships predicted by the IPA program were also examined (**Figure 7E**). Many of these networks are related to inflammatory signaling mechanisms, suggesting a link between pro-inflammatory signaling and synaptic transmission (Alexander and Popovich, 2009; Walters, 2014; Medelin et al., 2018). Previous work has associated inflammatory mechanisms to diseases of the CNS, including multiple sclerosis, Alzheimer's disease, and Parkinson's disease (Medelin et al., 2018). The mechanisms through which inflammation prompts changes in synaptic transmission are not fully understood, but several of the classic pro-inflammatory cytokines (including TNF-α, IL-6, IL-1β) have been shown to contribute to a decrease in hippocampal neurogenesis, and could be playing a similar role within the spinal cord following injury (Kohman and Rhodes, 2013). Overall, pro-inflammatory conditions have been associated with increases in post-synaptic NMDA and AMPA receptors, and inhibition of GABAergic receptors (Medelin et al., 2018).

CONCLUSION

Molecular changes typically reflect phenotypic characteristics, and our data show changes in gene expression 4 days after injury, suggesting that many of these genes may be responsible for the

development of spontaneous activity reported elsewhere (Bedi et al., 2010; Yang et al., 2014). We recognize that RNA-Seq of batched neurons elucidated changes in gene targets in a subpopulation of cells, but averaging occurred when pooling large numbers of cells, precluding analysis at the level of the single cell (Haque et al., 2017). Further analysis at the single-cell level of cutaneous nociceptors will clarify the contributions of specific subpopulations (non-peptidergic vs. peptidergic) to chronic pain after SCI. Functional studies are also needed to analyze the roles of this specific cell population, to better understand the connectivity and plasticity of the CNS and PNS. While our results begin to address prospective gene networks that may contribute to the development of chronic pain, additional behavioral testing in conjunction with targeting of specific biological mechanisms until the chronic pain phase is necessary in order to attribute specific transcriptional changes to pain phenotypes. The DRG nociceptor preparation isolated by backlabeling with WGA-488 and FACS has many applications in molecular studies. However, it is important to note that while this methodology is beneficial in gaining knowledge of changes in gene expression at the transcriptional level, additional studies would need to be done to corroborate similar changes in protein levels. Previously mentioned isolation methods such as TRAP-seq are able to elucidate functional changes at the translational level. We have demonstrated how the cutaneous nociceptor transcriptome is altered following SCI to gain novel biological insight into disease mechanisms in a cell-type-specific approach. It is evident that the transition from acute to chronic pain occurs in distinct steps that involve numerous signaling pathways, providing a host of potential new drug targets.

DATA AVAILABILITY STATEMENT

The datasets generated during and/or analyzed during the current study are available in Gene Expression Omnibus (GEO) repository under the series record number GSE132552, all other data generated during this study are included in this published article (and its **Supplementary Material**).

ETHICS STATEMENT

The animal study was reviewed and approved by University of Connecticut health Center Institutional Animal Care and Use Committee.

AUTHOR CONTRIBUTIONS

JY and RM designed the research. JY performed the research. JY and RM analyzed the data. JY, IM and RM wrote the article.

FUNDING

This work was supported by National Institutes of Health (NIH) DK032948 (RM) and the University of Connecticut Graduate School. Both played no role in the any decisions about scientific direction or judgments.

ACKNOWLEDGMENTS

We thank Dr. Nicholas Wasko and Dr. Robert Clarke for providing us with cuprizone-treated mice, and Dr. Evan Jellison for his help and expertise with flow cytometry. We acknowledge Dr. Bo Reese and the Center for Genome Innovation, Institute for Systems Genomics, University of Connecticut for library construction and RNA sequencing services. We also acknowledge Dr. Vijender Singh and the Computational Biology Core, Institute for Systems Genomics, University of Connecticut for base-calling, read alignment, and assembly of individual transcripts to align to the genome.

SUPPLEMENTARY MATERIAL

The Supplementary Material for this article can be found online at: https://www.frontiersin.org/articles/10.3389/fnmol.2019.00284/full#supplementary-material.

REFERENCES

Alexander, J. K., and Popovich, P. G. (2009). Neuroinflammation in spinal cord injury: therapeutic targets for neuroprotection and regeneration. *Prog. Brain Res.* 175, 125–137. doi: 10.1016/s0079-6123(09)17508-8

Baek, A., Cho, S. R., and Kim, S. H. (2017). Elucidation of gene expression patterns in the brain after spinal cord injury. *Cell Transplant.* 26, 1286–1300. doi: 10.1177/0963689717715822

Bannon, A. W., and Malmberg, A. B. (2007). Models of nociception: hot-plate, tail-flick, and formalin tests in rodents. *Curr. Protoc. Neurosci.* 8:8.9. doi: 10.1002/0471142301.ns0809s41

Basbaum, A. I., Bautista, D. M., Scherrer, G., and Julius, D. (2009). Cellular and molecular mechanisms of pain. *Cell* 139, 267–284. doi: 10.1016/j.cell.2009.09.028

Basso, D. M., Fisher, L. C., Anderson, A. J., Jakeman, L. B., McTigue, D. M., and Popovich, P. G. (2006). Basso mouse scale for locomotion detects differences in recovery after spinal cord injury in five common mouse strains. *J. Neurotrauma* 23, 635–659. doi: 10.1089/neu.2006.23.635

Bedi, S. S., Yang, Q., Crook, R. J., Du, J., Wu, Z., Fishman, H. M., et al. (2010). Chronic spontaneous activity generated in the somata of primary nociceptors is associated with pain-related behavior after spinal cord injury. *J. Neurosci.* 30, 14870–14882. doi: 10.1523/JNEUROSCI.2428-10.2010

Berta, T., Perrin, F. E., Pertin, M., Tonello, R., Liu, Y. C., Chamessian, A., et al. (2017). Gene expression profiling of cutaneous injured and non-injured nociceptors in SNI animal model of neuropathic pain. *Sci. Rep.* 7:9367. doi: 10.1038/s41598-017-08865-3

Biederer, T., and Stagi, M. (2008). Signaling by synaptogenic molecules. *Curr. Opin. Neurobiol.* 18, 261–269. doi: 10.1016/j.conb.2008.07.014

Bruce, J. C., Oatway, M. A., and Weaver, L. C. (2002). Chronic pain after clip-compression injury of the rat spinal cord. *Exp. Neurol.* 178, 33–48. doi: 10.1006/exnr.2002.8026

Buch, N. S., Ahlburg, P., Haroutounian, S., Andersen, N. T., Finnerup, N. B., and Nikolajsen, L. (2019). The role of afferent input in postamputation pain: a randomized, double-blind, placebo-controlled crossover study. *Pain* 160, 1622–1633. doi: 10.1097/j.pain.0000000000001536

Bundesen, L. Q., Scheel, T. A., Bregman, B. S., and Kromer, L. F. (2003). Ephrin-B2 and EphB2 regulation of astrocyte-meningeal fibroblast interactions in response to spinal cord lesions in adult rats. *J. Neurosci.* 23, 7789–7800. doi: 10.1523/JNEUROSCI.23-21-07789.2003

Campbell, J. N., Raja, S. N., Meyer, R. A., and Mackinnon, S. E. (1988). Myelinated afferents signal the hyperalgesia associated with nerve injury. *Pain* 32, 89–94. doi: 10.1016/0304-3959(88)90027-9

Cardenas, D. D., Bryce, T. N., Shem, K., Richards, J. S., and Elhefni, H. (2004). Gender and minority differences in the pain experience of people with spinal cord injury. *Arch. Phys. Med. Rehabil.* 85, 1774–1781. doi: 10.1310/kg8c-tjcp-95a5-n949

Carlton, S. M., Du, J., Tan, H. Y., Nesic, O., Hargett, G. L., Bopp, A. C., et al. (2009). Peripheral and central sensitization in remote spinal cord regions contribute to central neuropathic pain after spinal cord injury. *Pain* 147, 265–276. doi: 10.1016/j.pain.2009.09.030

Chiu, I. M., Barrett, L. B., Williams, E. K., Strochlic, D. E., Lee, S., Weyer, A. D., et al. (2014). Transcriptional profiling at whole population and single cell levels reveals somatosensory neuron molecular diversity. *Elife* 3:e04660. doi: 10.7554/eLife.04660

Christensen, M. D., and Hulsebosch, C. E. (1997). Chronic central pain after spinal cord injury. *J. Neurotrauma* 14, 517–537. doi: 10.1089/neu.1997.14.517

Citri, A., Pang, Z. P., Sudhof, T. C., Wernig, M., and Malenka, R. C. (2011). Comprehensive qPCR profiling of gene expression in single neuronal cells. *Nat. Protoc.* 7, 118–127. doi: 10.1038/nprot.2011.430

Conesa, A., Madrigal, P., Tarazona, S., Gomez-Cabrero, D., Cervera, A., McPherson, A., et al. (2016). A survey of best practices for RNA-seq data analysis. *Genome Biol.* 17:13. doi: 10.1186/s13059-016-0881-8

Cook, A. D., Christensen, A. D., Tewari, D., McMahon, S. B., and Hamilton, J. A. (2018). Immune cytokines and their receptors in inflammatory pain. *Trends Immunol.* 39, 240–255. doi: 10.1016/j.it.2017.12.003

da Silva Serra, I., Husson, Z., Bartlett, J. D., and Smith, E. S. (2016). Characterization of cutaneous and articular sensory neurons. *Mol. Pain* 12:1744806916636387. doi: 10.1177/1744806916636387

Davoody, L., Quiton, R. L., Lucas, J. M., Ji, Y., Keller, A., and Masri, R. (2011). Conditioned place preference reveals tonic pain in an animal model of central pain. *J. Pain* 12, 868–874. doi: 10.1016/j.jpain.2011.01.010

de Hoon, M. J., Imoto, S., Nolan, J., and Miyano, S. (2004). Open source clustering software. *Bioinformatics* 20, 1453–1454. doi: 10.1093/bioinformatics/bth078

De Jongh, R. F., Vissers, K. C., Meert, T. F., Booij, L. H., De Deyne, C. S., and Heylen, R. J. (2003). The role of interleukin-6 in nociception and pain. *Anesth. Analg.* 96, 1096–1103. doi: 10.1213/01.ane.0000055362.56604.78

Defrin, R., Ohry, A., Blumen, N., and Urca, G. (2001). Characterization of chronic pain and somatosensory function in spinal cord injury subjects. *Pain* 89, 253–263. doi: 10.1016/s0304-3959(00)00369-9

Deng, X., Wang, D., Wang, S., Wang, H., and Zhou, H. (2018). Identification of key genes and pathways involved in response to pain in goat and sheep by transcriptome sequencing. *Biol. Res.* 51:25. doi: 10.1186/s40659-018-0174-7

Densmore, V. S., Kalous, A., Keast, J. R., and Osborne, P. B. (2010). Above-level mechanical hyperalgesia in rats develops after incomplete spinal cord injury but not after cord transection and is reversed by amitriptyline, morphine and gabapentin. *Pain* 151, 184–193. doi: 10.1016/j.pain.2010.07.007

Devor, M. (2006). Sodium channels and mechanisms of neuropathic pain. *J. Pain* 7, S3–S12. doi: 10.1016/j.jpain.2005.09.006

Devor, M. (2009). Ectopic discharge in Aβ afferents as a source of neuropathic pain. *Exp. Brain Res.* 196, 115–128. doi: 10.1007/s00221-009-1724-6

Dixon, W. J. (1980). Efficient analysis of experimental observations. *Annu. Rev. Pharmacol. Toxicol.* 20, 441–462. doi: 10.1146/annurev.pa.20.040180.002301

Djouhri, L., Dawbarn, D., Robertson, A., Newton, R., and Lawson, S. N. (2001). Time course and nerve growth factor dependence of inflammation-induced alterations in electrophysiological membrane properties in nociceptive primary afferent neurons. *J. Neurosci.* 21, 8722–8733. doi: 10.1523/JNEUROSCI.21-22-08722.2001

Dominguez, E., Rivat, C., Pommier, B., Mauborgne, A., and Pohl, M. (2008). JAK/STAT3 pathway is activated in spinal cord microglia after peripheral nerve injury and contributes to neuropathic pain development in rat. *J. Neurochem.* 107, 50–60. doi: 10.1111/j.1471-4159.2008.05566.x

Donnelly, D. J., and Popovich, P. G. (2008). Inflammation and its role in neuroprotection, axonal regeneration and functional recovery after spinal cord injury. *Exp. Neurol.* 209, 378–388. doi: 10.1016/j.expneurol.2007.06.009

Dubner, R., and Ruda, M. A. (1992). Activity-dependent neuronal plasticity following tissue injury and inflammation. *Trends Neurosci.* 15, 96–103. doi: 10.1016/0166-2236(92)90019-5

Eijkelkamp, N., Linley, J. E., Torres, J. M., Bee, L., Dickenson, A. H., Gringhuis, M., et al. (2013). A role for Piezo2 in EPAC1-dependent mechanical allodynia. *Nat. Commun.* 4:1682. doi: 10.1038/ncomms2673

Finnerup, N. B., Johannesen, I. L., Sindrup, S. H., Bach, F. W., and Jensen, T. S. (2001). Pain and dysesthesia in patients with spinal cord injury: a postal survey. *Spinal Cord* 39, 256–262. doi: 10.1038/sj.sc.3101161

Gallego Romero, I., Pai, A. A., Tung, J., and Gilad, Y. (2014). RNA-seq: impact of RNA degradation on transcript quantification. *BMC Biol.* 12:42. doi: 10.1186/1741-7007-12-42

Gaudet, A. D., Ayala, M. T., Schleicher, W. E., Smith, E. J., Bateman, E. M., Maier, S. F., et al. (2017). Exploring acute-to-chronic neuropathic pain in rats after contusion spinal cord injury. *Exp. Neurol.* 295, 46–54. doi: 10.1016/j.expneurol.2017.05.011

Gold, M. S., and Gebhart, G. F. (2010). Nociceptor sensitization in pain pathogenesis. *Nat. Med.* 16, 1248–1257. doi: 10.1038/nm.2235

Goswami, S. C., Mishra, S. K., Maric, D., Kaszas, K., Gonnella, G. L., Clokie, S. J., et al. (2014). Molecular signatures of mouse TRPV1-lineage neurons revealed by RNA-Seq transcriptome analysis. *J. Pain* 15, 1338–1359. doi: 10.1016/j.jpain.2014.09.010

Guptarak, J., Wanchoo, S., Durham-Lee, J., Wu, Y., Zivadinovic, D., Paulucci-Holthauzen, A., et al. (2013). Inhibition of IL-6 signaling: a novel therapeutic approach to treating spinal cord injury pain. *Pain* 154, 1115–1128. doi: 10.1016/j.pain.2013.03.026

Haque, A., Engel, J., Teichmann, S. A., and Lonnberg, T. (2017). A practical guide to single-cell RNA-sequencing for biomedical research and clinical applications. *Genome Med.* 9:75. doi: 10.1186/s13073-017-0467-4

Haroutounian, S., Ford, A. L., Frey, K., Nikolajsen, L., Finnerup, N. B., Neiner, A., et al. (2018). How central is central poststroke pain? The role of afferent input in poststroke neuropathic pain: a prospective, open-label pilot study. *Pain* 159, 1317–1324. doi: 10.1097/j.pain.0000000000001213

Harriott, A. M., and Gold, M. S. (2009). Contribution of primary afferent channels to neuropathic pain. *Curr. Pain Headache Rep.* 13, 197–207. doi: 10.1007/s11916-009-0034-9

Harris, J. A. (1998). Using c-fos as a neural marker of pain. *Brain Res. Bull.* 45, 1–8. doi: 10.1016/s0361-9230(97)00277-3

Hu, G., Huang, K., Hu, Y., Du, G., Xue, Z., Zhu, X., et al. (2016). Single-cell RNA-seq reveals distinct injury responses in different types of DRG sensory neurons. *Sci. Rep.* 6:31851. doi: 10.1038/srep31851

Huang, L. Y., Gu, Y., and Chen, Y. (2013). Communication between neuronal somata and satellite glial cells in sensory ganglia. *Glia* 61, 1571–1581. doi: 10.1002/glia.22541

Huang, W. L., Robson, D., Liu, M. C., King, V. R., Averill, S., Shortland, P. J., et al. (2006). Spinal cord compression and dorsal root injury cause up-regulation of activating transcription factor-3 in large-diameter dorsal root ganglion neurons. *Eur. J. Neurosci.* 23, 273–278. doi: 10.1111/j.1460-9568.2005.04530.x

Joshi, M., and Fehlings, M. G. (2002). Development and characterization of a novel, graded model of clip compressive spinal cord injury in the mouse: Part 1. Clip design, behavioral outcomes and histopathology. *J. Neurotrauma* 19, 175–190. doi: 10.1089/08977150252806947

Julius, D., and Basbaum, A. I. (2001). Molecular mechanisms of nociception. *Nature* 413, 203–210. doi: 10.1038/35093019

Khangura, R. K., Sharma, J., Bali, A., Singh, N., and Jaggi, A. S. (2019). An integrated review on new targets in the treatment of neuropathic pain. *Korean J. Physiol. Pharmacol.* 23, 1–20. doi: 10.4196/kjpp.2019.23.1.1

Kjell, J., and Olson, L. (2016). Rat models of spinal cord injury: from pathology to potential therapies. *Dis. Model. Mech.* 9, 1125–1137. doi: 10.1242/dmm.025833

Klein, R. (2004). Eph/ephrin signaling in morphogenesis, neural development and plasticity. *Curr. Opin. Cell Biol.* 16, 580–589. doi: 10.1016/j.ceb.2004.07.002

Klenke, S., Renckhoff, K., Engler, A., Peters, J., and Frey, U. H. (2016). Easy-to-use strategy for reference gene selection in quantitative real-time PCR experiments. *Naunyn Schmiedebergs. Arch. Pharmacol.* 389, 1353–1366. doi: 10.1007/s00210-016-1305-8

Kobayashi, H., Kitamura, T., Sekiguchi, M., Homma, M. K., Kabuyama, Y., Konno, S., et al. (2007). Involvement of EphB1 receptor/EphrinB2 ligand in neuropathic pain. *Spine* 32, 1592–1598. doi: 10.1097/brs.0b013e318074d46a

Kohman, R. A., and Rhodes, J. S. (2013). Neurogenesis, inflammation and behavior. *Brain Behav. Immun.* 27, 22–32. doi: 10.1016/j.bbi.2012.09.003

Kramer, J. L., Minhas, N. K., Jutzeler, C. R., Erskine, E. L., Liu, L. J., and Ramer, M. S. (2017). Neuropathic pain following traumatic spinal cord injury: models, measurement, and mechanisms. *J. Neurosci. Res.* 95, 1295–1306. doi: 10.1002/jnr.23881

Krames, E. S. (2014). The role of the dorsal root ganglion in the development of neuropathic pain. *Pain Med.* 15, 1669–1685. doi: 10.1111/pme.12413

Labaj, P. P., and Kreil, D. P. (2016). Sensitivity, specificity and reproducibility of RNA-Seq differential expression calls. *Biol. Direct* 11:66. doi: 10.1186/s13062-016-0169-7

Lallemend, F., and Ernfors, P. (2012). Molecular interactions underlying the specification of sensory neurons. *Trends Neurosci.* 35, 373–381. doi: 10.1016/j.tins.2012.03.006

Le Pichon, C. E., and Chesler, A. T. (2014). The functional and anatomical dissection of somatosensory subpopulations using mouse genetics. *Front. Neuroanat.* 8:21. doi: 10.3389/fnana.2014.00021

Lima, L., Gaiteiro, C., Peixoto, A., Soares, J., Neves, M., Santos, L. L., et al. (2016). Reference genes for addressing gene expression of bladder cancer cell models under hypoxia: a step towards transcriptomic studies. *PLoS One* 11:e0166120. doi: 10.1371/journal.pone.0166120

Lopes, D. M., Denk, F., and McMahon, S. B. (2017). The molecular fingerprint of dorsal root and trigeminal ganglion neurons. *Front. Mol. Neurosci.* 10:304. doi: 10.3389/fnmol.2017.00304

Love, M. I., Huber, W., and Anders, S. (2014). Moderated estimation of fold change and dispersion for RNA-seq data with DESeq2. *Genome Biol.* 15:550. doi: 10.1186/s13059-014-0550-8

Lu, B., Wang, K. H., and Nose, A. (2009). Molecular mechanisms underlying neural circuit formation. *Curr. Opin. Neurobiol.* 19, 162–167. doi: 10.1016/j.conb.2009.04.004

Ma, M., Basso, D. M., Walters, P., Stokes, B. T., and Jakeman, L. B. (2001). Behavioral and histological outcomes following graded spinal cord contusion injury in the C57Bl/6 mouse. *Exp. Neurol.* 169, 239–254. doi: 10.1006/exnr.2001.7679

Mains, R. E., Blaby-Haas, C., Rheaume, B. A., and Eipper, B. A. (2018). Changes in corticotrope gene expression upon increased expression of peptidylglycine α-amidating monooxygenase. *Endocrinology* 159, 2621–2639. doi: 10.1210/en.2018-00235

Malin, S. A., Davis, B. M., and Molliver, D. C. (2007). Production of dissociated sensory neuron cultures and considerations for their use in studying neuronal function and plasticity. *Nat. Protoc.* 2, 152–160. doi: 10.1038/nprot.2006.461

Marques, S. A., de Almeida, F. M., Mostacada, K., and Martinez, A. M. (2014). A highly reproducible mouse model of compression spinal cord injury. *Methods Mol. Biol.* 1162, 149–156. doi: 10.1007/978-1-4939-0777-9_12

Medelin, M., Giacco, V., Aldinucci, A., Castronovo, G., Bonechi, E., Sibilla, A., et al. (2018). Bridging pro-inflammatory signals, synaptic transmission and protection in spinal explants *in vitro*. *Mol. Brain* 11:3. doi: 10.1186/s13041-018-0347-x

Megat, S., Ray, P. R., Tavares-Ferreira, D., Moy, J. K., Sankaranarayanan, I., Wanghzou, A., et al. (2019). Differences between dorsal root and trigeminal ganglion nociceptors in mice revealed by translational profiling. *J. Neurosci.* 39, 6829–6847. doi: 10.1523/jneurosci.2663-18.2019

Meisner, J. G., Marsh, A. D., and Marsh, D. R. (2010). Loss of GABAergic interneurons in laminae I-III of the spinal cord dorsal horn contributes to reduced GABAergic tone and neuropathic pain after spinal cord injury. *J. Neurotrauma* 27, 729–737. doi: 10.1089/neu.2009.1166

Melemedjian, O. K., Tillu, D. V., Asiedu, M. N., Mandell, E. K., Moy, J. K., Blute, V. M., et al. (2013). BDNF regulates atypical PKC at spinal synapses to initiate and maintain a centralized chronic pain state. *Mol. Pain* 9:12. doi: 10.1186/1744-8069-9-12

Mueller, O., Lightfoot, S., and Schroeder, A. (2016). *RNA Integrity Number (RIN)—Standardization of RNA Quality Control.* Waldbronn: Agilent Technologies.

Mukhamedshina, Y. O., Akhmetzyanova, E. R., Martynova, E. V., Khaiboullina, S. F., Galieva, L. R., and Rizvanov, A. A. (2017). Systemic and local cytokine profile following spinal cord injury in rats: a multiplex analysis. *Front. Neurol.* 8:581. doi: 10.3389/fneur.2017.00581

Nakae, A., Nakai, K., Yano, K., Hosokawa, K., Shibata, M., and Mashimo, T. (2011). The animal model of spinal cord injury as an experimental pain model. *J. Biomed. Biotechnol.* 2011:939023. doi: 10.1155/2011/939023

Naranjo, J. R., Mellstrom, B., Achaval, M., and Sassone-Corsi, P. (1991). Molecular pathways of pain: Fos/Jun-mediated activation of a noncanonical AP-1 site in the prodynorphin gene. *Neuron* 6, 607–617. doi: 10.1016/0896-6273(91)90063-6

Nees, T. A., Tappe-Theodor, A., Sliwinski, C., Motsch, M., Rupp, R., Kuner, R., et al. (2016). Early-onset treadmill training reduces mechanical allodynia and modulates calcitonin gene-related peptide fiber density in lamina III/IV in a mouse model of spinal cord contusion injury. *Pain* 157, 687–697. doi: 10.1097/j.pain.0000000000000422

Odem, M. A., Bavencoffe, A. G., Cassidy, R. M., Lopez, E. R., Tian, J., Dessauer, C. W., et al. (2018). Isolated nociceptors reveal multiple specializations for generating irregular ongoing activity associated with ongoing pain. *Pain* 159, 2347–2362. doi: 10.1097/j.pain.0000000000001341

Odem, M. A., Lacagnina, M. J., Katzen, S. L., Li, J., Spence, E. A., Grace, P. M., et al. (2019). Sham surgeries for central and peripheral neural injuries persistently enhance pain-avoidance behavior as revealed by an operant conflict test. *Pain* 160, 2440–2455. doi: 10.1097/j.pain.0000000000001642

Price, T. J., and Inyang, K. E. (2015). Commonalities between pain and memory mechanisms and their meaning for understanding chronic pain. *Prog. Mol. Biol. Transl. Sci.* 131, 409–434. doi: 10.1016/bs.pmbts.2014.11.010

Ramabadran, K., Bansinath, M., Turndorf, H., and Puig, M. M. (1989). Tail immersion test for the evaluation of a nociceptive reaction in mice. *J. Pharmacol. Methods* 21, 21–31. doi: 10.1016/0160-5402(89)90019-3

Ritter, D. M., Zemel, B. M., Lepore, A. C., and Covarrubias, M. (2015). Kv3.4 channel function and dysfunction in nociceptors. *Channels* 9, 209–217. doi: 10.1080/19336950.2015.1056949

Schmitz, T., and Chew, L. J. (2008). Cytokines and myelination in the central nervous system. *ScientificWorldJournal* 8, 1119–1147. doi: 10.1100/tsw.2008.140

Schroeder, A., Mueller, O., Stocker, S., Salowsky, R., Leiber, M., Gassmann, M., et al. (2006). The RIN: an RNA integrity number for assigning integrity values to RNA measurements. *BMC Mol. Biol.* 7:3. doi: 10.1186/1471-2199-7-3

Seijffers, R., Mills, C. D., and Woolf, C. J. (2007). ATF3 increases the intrinsic growth state of DRG neurons to enhance peripheral nerve regeneration. *J. Neurosci.* 27, 7911–7920. doi: 10.1523/JNEUROSCI.5313-06.2007

Shiao, R., and Lee-Kubli, C. A. (2018). Neuropathic pain after spinal cord injury: challenges and research perspectives. *Neurotherapeutics* 15, 635–653. doi: 10.1007/s13311-018-0633-4

Shields, S. D., Ahn, H. S., Yang, Y., Han, C., Seal, R. P., Wood, J. N., et al. (2012). Nav1.8 expression is not restricted to nociceptors in mouse peripheral nervous system. *Pain* 153, 2017–2030. doi: 10.1016/j.pain.2012.04.022

Siddall, P. J., and Loeser, J. D. (2001). Pain following spinal cord injury. *Spinal Cord* 39, 63–73. doi: 10.1038/sj.sc.3101116

Siddall, P. J., McClelland, J. M., Rutkowski, S. B., and Cousins, M. J. (2003). A longitudinal study of the prevalence and characteristics of pain in the first 5 years following spinal cord injury. *Pain* 103, 249–257. doi: 10.1016/s0304-3959(02)00452-9

Stammers, A. T., Liu, J., and Kwon, B. K. (2012). Expression of inflammatory cytokines following acute spinal cord injury in a rodent model. *J. Neurosci. Res.* 90, 782–790. doi: 10.1002/jnr.22820

Suzuki, K., and Kikkawa, Y. (1969). Status spongiosus of CNS and hepatic changes induced by cuprizone (biscyclohexanone oxalyldihydrazone). *Am. J. Pathol.* 54, 307–325.

Szczot, M., Liljencrantz, J., Ghitani, N., Barik, A., Lam, R., Thompson, J. H., et al. (2018). PIEZO2 mediates injury-induced tactile pain in mice and humans. *Sci. Transl. Med.* 10:eaat9892. doi: 10.1126/scitranslmed.aat9892

Tator, C. P., and Poon, P. (2008). "Acute clip impact-compression model," in *Animal Models of Acute Neurological Injuries*, eds J. Chen, Z. C. Xu, X.-M. Xu and J. H. Zhang (New York, NY and Totowa, NJ: Humana Press), 449–460.

Thakur, M., Crow, M., Richards, N., Davey, G. I., Levine, E., Kelleher, J. H., et al. (2014). Defining the nociceptor transcriptome. *Front. Mol. Neurosci.* 7:87. doi: 10.3389/fnmol.2014.00087

Tsuda, M., Kohro, Y., Yano, T., Tsujikawa, T., Kitano, J., Tozaki-Saitoh, H., et al. (2011). JAK-STAT3 pathway regulates spinal astrocyte proliferation and neuropathic pain maintenance in rats. *Brain* 134, 1127–1139. doi: 10.1093/brain/awr025

Tsujino, H., Kondo, E., Fukuoka, T., Dai, Y., Tokunaga, A., Miki, K., et al. (2000). Activating transcription factor 3 (ATF3) induction by axotomy in sensory and motoneurons: a novel neuronal marker of nerve injury. *Mol. Cell. Neurosci.* 15, 170–182. doi: 10.1006/mcne.1999.0814

Usoskin, D., Furlan, A., Islam, S., Abdo, H., Lonnerberg, P., Lou, D., et al. (2015). Unbiased classification of sensory neuron types by large-scale single-cell RNA sequencing. *Nat. Neurosci.* 18, 145–153. doi: 10.1038/nn.3881

Vaso, A., Adahan, H. M., Gjika, A., Zahaj, S., Zhurda, T., Vyshka, G., et al. (2014). Peripheral nervous system origin of phantom limb pain. *Pain* 155, 1384–1391. doi: 10.1016/j.pain.2014.04.018

Walters, E. T. (2012). Nociceptors as chronic drivers of pain and hyperreflexia after spinal cord injury: an adaptive-maladaptive hyperfunctional state hypothesis. *Front. Physiol.* 3:309. doi: 10.3389/fphys.2012.00309

Walters, E. T. (2014). Neuroinflammatory contributions to pain after SCI: roles for central glial mechanisms and nociceptor-mediated host defense. *Exp. Neurol.* 258, 48–61. doi: 10.1016/j.expneurol.2014.02.001

Walters, E. T. (2018). How is chronic pain related to sympathetic dysfunction and autonomic dysreflexia following spinal cord injury? *Auton. Neurosci.* 209, 79–89. doi: 10.1016/j.autneu.2017.01.006

Wang, H., and Zylka, M. J. (2009). Mrgprd-expressing polymodal nociceptive neurons innervate most known classes of substantia gelatinosa neurons. *J. Neurosci.* 29, 13202–13209. doi: 10.1523/jneurosci.3248-09.2009

Wasko, N. J., Kulak, M. H., Paul, D., Nicaise, A. M., Yeung, S. T., Nichols, F. C., et al. (2019). Systemic TLR2 tolerance enhances central nervous system remyelination. *J. Neuroinflammation* 16:158. doi: 10.1186/s12974-019-1540-2

Waxman, S. G., Dib-Hajj, S., Cummins, T. R., and Black, J. A. (1999). Sodium channels and pain. *Proc. Natl. Acad. Sci. U S A* 96, 7635–7639. doi: 10.1073/pnas.96.14.7635

Wickenden, A. (2002). K(+) channels as therapeutic drug targets. *Pharmacol. Ther.* 94, 157–182. doi: 10.1016/s0163-7258(02)00201-2

Woolf, C. J. (2011). Central sensitization: implications for the diagnosis and treatment of pain. *Pain* 152, S2–S15. doi: 10.1016/j.pain.2010.09.030

Wu, G., Ringkamp, M., Hartke, T. V., Murinson, B. B., Campbell, J. N., Griffin, J. W., et al. (2001). Early onset of spontaneous activity in uninjured C-fiber nociceptors after injury to neighboring nerve fibers. *J. Neurosci.* 21:RC140. doi: 10.1523/jneurosci.21-08-j0002.2001

Wu, Z., and Wu, H. (2016). Experimental design and power calculation for RNA-seq experiments. *Methods Mol. Biol.* 1418, 379–390. doi: 10.1007/978-1-4939-3578-9_18

Wu, Z., Yang, Q., Crook, R. J., O'Neil, R. G., and Walters, E. T. (2013). TRPV1 channels make major contributions to behavioral hypersensitivity and spontaneous activity in nociceptors after spinal cord injury. *Pain* 154, 2130–2141. doi: 10.1016/j.pain.2013.06.040

Xia, M., Liu, D., and Yao, C. (2015). TRPC3: a new target for therapeutic strategies in chronic pain-DAG-mediated activation of non-selective cation currents and chronic pain (Mol. Pain 2014;10:43). *J. Neurogastroenterol. Motil.* 21, 445–447. doi: 10.5056/jnm15078

Xie, W., Strong, J. A., Meij, J. T., Zhang, J. M., and Yu, L. (2005). Neuropathic pain: early spontaneous afferent activity is the trigger. *Pain* 116, 243–256. doi: 10.1016/j.pain.2005.04.017

Xue, Z. J., Shen, L., Wang, Z. Y., Hui, S. Y., Huang, Y. G., and Ma, C. (2014). STAT3 inhibitor WP1066 as a novel therapeutic agent for bCCI neuropathic pain rats. *Brain Res.* 1583, 79–88. doi: 10.1016/j.brainres.2014.07.015

Yan, X., Liu, J., Ye, Z., Huang, J., He, F., Xiao, W., et al. (2016). CaMKII-mediated CREB phosphorylation is involved in Ca^{2+}-induced BDNF mRNA transcription and neurite outgrowth promoted by electrical stimulation. *PLoS One* 11:e0162784. doi: 10.1371/journal.pone.0162784

Yang, Q., Wu, Z., Hadden, J. K., Odem, M. A., Zuo, Y., Crook, R. J., et al. (2014). Persistent pain after spinal cord injury is maintained by primary afferent activity. *J. Neurosci.* 34, 10765–10769. doi: 10.1523/JNEUROSCI.5316-13.2014

Yezierski, R. P. (2005). Spinal cord injury: a model of central neuropathic pain. *Neurosignals* 14, 182–193. doi: 10.1159/000087657

You, H. J., Colpaert, F. C., and Arendt-Nielsen, L. (2008). Long-lasting descending and transitory short-term spinal controls on deep spinal dorsal horn nociceptive-specific neurons in response to persistent nociception. *Brain Res. Bull.* 75, 34–41. doi: 10.1016/j.brainresbull.2007.07.015

Zhang, D., Mou, J. Y., Wang, F., Liu, J., and Hu, X. (2019). CRNDE enhances neuropathic pain *via* modulating miR-136/IL6R axis in CCI rat models. *J. Cell. Physiol.* 234, 22234–22241. doi: 10.1002/jcp.28790

Zhou, Q., Bao, Y., Zhang, X., Zeng, L., Wang, L., Wang, J., et al. (2014). Optimal interval for hot water immersion tail-flick test in rats. *Acta Neuropsychiatr.* 26, 218–222. doi: 10.1017/neu.2013.57

Zylka, M. J., Rice, F. L., and Anderson, D. J. (2005). Topographically distinct epidermal nociceptive circuits revealed by axonal tracers targeted to Mrgprd. *Neuron* 45, 17–25. doi: 10.1016/j.neuron.2004.12.015

Conflict of Interest: The authors declare that the research was conducted in the absence of any commercial or financial relationships that could be construed as a potential conflict of interest.